Cell Biology
Developmental Biology

Female-germline specific protein Sakura interacts with Otu and is crucial for germline stem cell renewal and differentiation and oogenesis

Azali Azlan, Li Zhu, Ryuya Fukunaga

Department of Biological Chemistry, Johns Hopkins School of Medicine, Baltimore, United States

Reviewed Preprint
v3 • July 3, 2025
Revised by authors

Reviewed Preprint
v2 • June 13, 2025

Reviewed Preprint
v1 • November 27, 2024

eLife Assessment

This **valuable** study reports the first characterization of the CG14545 gene in Drosophila melanogaster, which the authors name "Sakura." Acting during germline stem cell fate and differentiation, Sakura is required for both oogenesis and female fertility, although some mechanistic details require further investigation. This **solid** study presents a wide-ranging and well-controlled characterization of Sakura, and accordingly the findings and associated reagents described will be of use to scientists interested in oogenesis and early development.

https://doi.org/10.7554/eLife.103828.3.sa4

Abstract

During oogenesis, self-renewal and differentiation of germline stem cells (GSCs) must be tightly regulated. The *Drosophila* female germline serves as an excellent model for studying these regulatory mechanisms. Here, we report that a previously uncharacterized gene *CG14545*, which we named *sakura*, is essential for oogenesis and female fertility in *Drosophila*. Sakura is predominantly expressed in the ovaries, particularly in the germline cells, including GSCs. *sakura* null mutant female flies display rudimentary ovaries with germline-less and tumorous phenotypes, fail to produce eggs, and are completely sterile. The germline-specific depletion of *sakura* impairs Dpp/BMP signaling, leading to aberrant *bag-of-marbles* (*bam*) expression, resulting in faulty differentiation and loss of GSCs. *sakura* is also necessary for normal levels of piwi-interacting RNAs (piRNAs) levels and for female-specific splicing of *sex-lethal* (*sxl*), a master regulator of sex identity determination. We identified Ovarian Tumor (Otu) as a protein binding partner of Sakura and found that loss of *otu* phenocopies loss of *sakura* in ovaries. Thus, we identify Sakura as a crucial factor for GSC renewal and differentiation and oogenesis, and propose that Sakura and Otu function together in these processes.

Introduction

Oogenesis is a complex process in which germline stem cells (GSCs) develop into mature female gametes or oocytes. This process involves multiple layers of regulations and numerous genes, some of which remain to be discovered and characterized. *Drosophila melanogaster*, a genetically tractable model organism, has long been at the forefront of GSC and oogenesis research (Kirilly and Xie 2007).

Adult *Drosophila* females possess a pair of ovaries, each composed of 12-16 ovarioles. At the anterior tip of each ovariole is a structure called the germarium, which houses two to three GSCs (**Fig 1A**). GSCs reside in the most anterior region of the germarium, where they directly contact cap cells and escort cells, forming a niche crucial for GSC self-renewal (Lin and Spradling 1993; de Cuevas and Matunis 2011; Losick et al. 2011). GSCs undergo asymmetric mitotic division, producing two distinct cells: one GSC and one cystoblast. The cystoblast, destined to differentiate, undergoes four mitotic divisions with incomplete cytokinesis, resulting in interconnected cysts of 2, 4, 8, and 16 cells. Of the 16 cells, one will differentiate into an oocyte, while the remaining 15 develop into polyploid nurse cells, which synthesize proteins and RNAs for deposition into the oocyte.

GSCs must be tightly regulated to maintain their undifferentiated state while dividing and differentiating to produce one GSC and one cystoblast. Failure in GSC self-renewal or inappropriate differentiation leads to stem cell loss, disrupting oocyte production (Lin 1997; Cox et al. 1998). Conversely, uncontrolled GSC division or defective differentiation results in an overabundance of GSC-like cells (a tumorous phenotype) and fewer differentiated cells, ultimately inhibiting oocyte production (Gateff et al. 1996; Ohlstein et al. 2000). Thus, a precise balance between GSC self-renewal and cyst differentiation within the germarium is essential for proper oogenesis and is tightly regulated.

Bone Morphogenetic Protein (BMP) signaling plays a critical role in regulating GSC self-renewal and differentiation during *Drosophila* oogenesis. In the stem cell niche, GSCs are physically anchored to cap cells via adherens and gap junctions (Song et al. 2002; Gilboa et al. 2003). Cap cells secrete BMP ligands, such as Decapentaplegic (Dpp) and Glass bottom boat (Gbb), which are recognized by transducing receptors like Thickvein (Tkv) and Saxophone (Sax) on the GSCs (Xie and Spradling 1998; Casanueva and Ferguson 2004). Upon activation, these receptors phosphorylate a transcription factor Mad. The phosphorylated Mad (pMad) translocates into the nucleus, where it represses the transcription of *bag-of-marbles* (*bam*), a key differentiation factor (Kai and Spradling 2003; Song et al. 2004).

Bam, a ubiquitin-associated protein, is essential for cystoblast differentiation (McKearin and Spradling 1990; McKearin and Ohlstein 1995). Dpp/BMP signaling in the niche represses *bam* expression, preventing GSCs from differentiating and enabling self-renew (Song et al. 2004). However, as the daughter cells (cytoblasts) exit the niche, they derepress *bam* and initiate the differentiation program. Tight regulation of Dpp/BMP signaling and *bam* expression ensures that only cells within the niche adopt GSC fate, while adjacent daughter cells differentiate into cystoblasts. Loss of *bam* leads to blocked differentiation and the accumulation of GSC-like cells (tumorous phenotype), whereas ectopic *bam* expression forces GSCs differentiation, depleting the stem cell pool (McKearin and Spradling 1990; McKearin and Ohlstein 1995; Ohlstein and McKearin 1997).

One of the proteins that interacts with Bam is Ovarian Tumor (Otu) (Ji et al. 2017). Otu forms a deubiquitinase complex with Bam, which deubiquitinates Cyclin A (CycA), stabilizing CycA and promoting GSC differentiation (Ji et al. 2017). Otu also binds RNAs (Ji et al. 2019). Otu is crucial

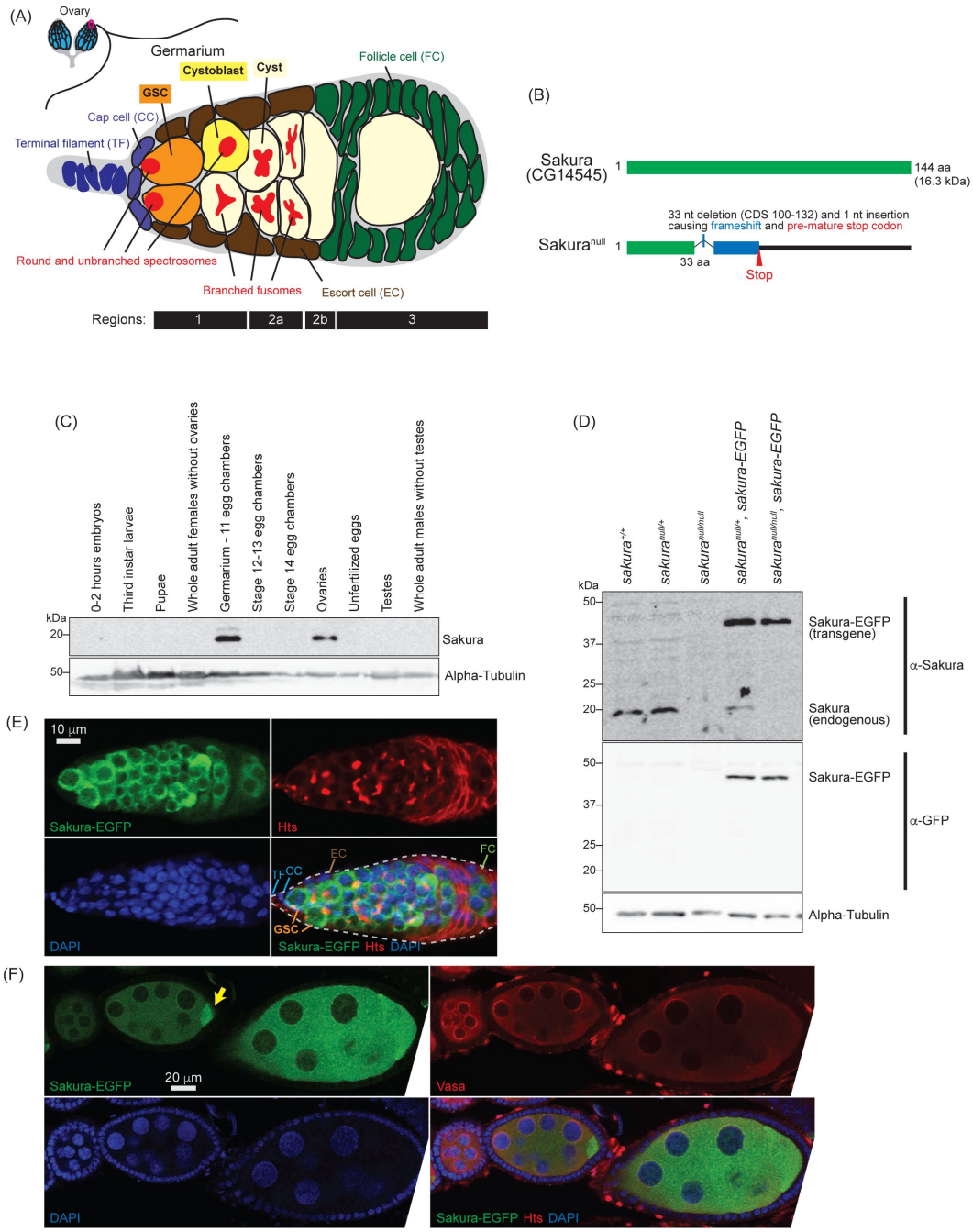

Fig 1.

Sakura expression pattern and mutant allele

(A) Schematic illustration of *Drosophila* ovary and germarium. *Drosophila* female has a pair of ovaries, each consisting of 12-16 ovarioles (cyan). The germarium (outlined with magenta) is located at the anterior tip of the ovarioles and consists of both germ cells and somatic cells. Germ cells include germline stem cells (GSCs), cystoblasts, cysts, and differentiating oocytes. Somatic cells include terminal filament (TF) cells, cap cells (CCc), escort cells (ECs), and follicle cells (FCs). GSCs and cystoblasts have spherical, unbranched spectrosomes, whereas cysts posesss branched fusomes. The distinct regions of the germarium —1, 2a, 2b, and 3—are indicated. (B) *Drosophila* Sakura protein (Sakura/CG14545) and its null mutant allele generated in this study. (C) Western blot of dissected fly tissues. (D) Western blot of ovary lysates. (E) Confocal images of the germarium from the *sakura-EGFP* transgenic fly. Sakura-EGFP (green), Hts (red), and DAPI (blue). Scale bar: 10 μm. (F) Confocal images of the egg chambers from the *sakura-EGFP* transgenic fly. Sakura-EGFP (green), Vasa (red), and DAPI (blue). Sakura-EGFP is expressed in nurse cells and enriched in the developing oocyte (yellow arrow). Scale bar: 20 μm.

for oogenesis and female fertility. Mutations in the *otu* gene cause various ovarian defects, including tumorous growths, germ cell loss, abnormalities in oocyte determination and nurse cell dumping, and defects in the sexual identity determination of germ cells, indicating Otu's importance in multiple stages of oogenesis (Smith and King 1966; Gans et al. 1975; Gollin and King 1981; King and Riley 1982; Storto and King 1988; Pauli et al. 1993; Rodesch et al. 1997; Glenn and Searles 2001). However, the precise molecular mechanisms by which Otu functions in these processes remain largely unknown.

In this study, we aimed to identify a novel gene required for oogenesis. Through a search for uncharacterized genes expressed exclusively in *Drosophila* ovaries, we discovered *CG14545*, a gene encoding a 114 amino acids (aa) long protein without any known functional domain (**Fig 1B**). We found that CG14545 is expressed specifically in female germline cells, including GSCs. Our genetic analysis revealed that *CG14545* is required for oogenesis and female fertility and plays an important intrinsic role in regulating GSCs renewal and differentiation. Additionally, CG14545 is important for the piRNA pathway and for the female-specific mRNA splicing pattern of *sex-lethal* (*sxl*), a master regulator of sex determination. We identified Otu as a binding partner of the CG14545 protein, suggesting that both proteins may participate in the same molecular pathways to regulate GSC fate and differentiation. We named the *CG14545* gene *sakura*, meaning "cherry blossom" in Japanese, symbolizing birth and renewal.

Results

Sakura is exclusively expressed in the ovaries

Based on high-throughput expression data in Flybase, *sakura* mRNA is highly and exclusively expressed in adult ovaries (**Fig S1**). To investigate Sakura protein expression, we generated a polyclonal anti-Sakura antibody against a recombinant full-length Sakura protein. Using this antibody, we examine Sakura protein expression at different stages of *Drosophila* development and across tissues. We found that Sakura protein is specifically expressed in ovaries, particularly in germarium - 11 egg chambers (**Fig 1C**).

sakura mutant flies

To explore the biological and molecular functions of Sakura *in vivo*, we generated a *sakura* mutant allele ($sakura^{null}$) with a one nucleotide (nt) insertion replacing 33 nts within the Sakura coding region using the CRISPR/Cas9 genome editing system (**Fig 1B**). This mutation causes a frameshift and a premature stop codon, resulting in a 33-amino acid (aa) N-terminal fragment of Sakura followed by a 22-aa segment produced by frameshifted translation (**Fig 1B**). This truncated fragment is unlikely to be functional, and we were unable to detect stable protein expression, as shown below (**Fig 1D**). Thus, we consider this allele a null mutation. $sakura^{null/null}$ flies were viable, revealing that Sakura is not essential for survival.

To validate the $sakura^{null}$ strain, we performed Western blots using ovary lysates from *sakura* mutant flies using the anti-Sakura antibody. As expected, full-length Sakura protein was detected in the ovaries of wild-type ($sakura^{+/+}$) and heterozygous controls ($sakura^{null/+}$), but not in those of homozygous mutants ($sakura^{null/null}$) (**Fig 1D**). No smaller protein corresponding to the truncated Sakura fragment was detected in either $sakura^{null/+}$ or $sakura^{null/null}$ ovaries thus, suggesting that the fragment is unstable or not expressed.

Sakura is cytoplasmic and expressed specifically in germ cells

To determine the localization of Sakura protein within the ovaries, we generated transgenic flies carrying a Sakura coding sequence fused with EGFP at the C-terminus (Sakura-EGFP) under the control of the *sakura* promoter. Western blot analysis of ovary lysates showed that Sakura-EGFP is

expressed at levels comparable to endogenous Sakura (**Fig 1D**).

Oogenesis begins in the germarium, which contains 2-3 GSCs identified by round, unbranched spectrosomes that contact cap cells (**Fig 1A**) (Kirilly and Xie 2007). In contrast, cysts exhibit branched fusomes. Immunostaining with hu-li tai shao (HTS) antibody marks both spectrosomes and fusomes (**Fig 1E**), while Vasa is a known germ cell marker (**Fig 1F**). Confocal imaging revealed that Sakura-EGFP is specifically expressed in the cytoplasm of germ cells, including GSCs, cyst cells, nurse cells, and developing oocytes (**Fig 1E** and **1F**). Sakura-EGFP was not expressed in somatic cells such as terminal filament, cap cells, escort cells, or follicle cells. (**Fig 1E**). In the egg chamber, Sakura-EGFP was detected in the cytoplasm of nurse cells and was enriched in developing oocytes (**Fig 1F**).

sakura is essential for female fertility

Given its ovary-specific expression at both mRNA and protein levels (**Fig 1C** and **S2**), we hypothesized that Sakura plays a critical role in ovarian function. Fertility assays revealed that $sakura^{null/null}$females laid no eggs when mated with wild-type males, while control females ($sakura^{+/+}$ and $sakura^{null/+}$) laid numerous eggs (**Fig 2A** and **2B**). Dissection of $sakura^{null/null}$ ovaries revealed that they were rudimentary compared to normal ovaries in controls (**Fig 2C**). This suggests that the inability of $sakura^{null/null}$ female to lay eggs is due to their underdeveloped ovaries. In contrast, $sakura^{null/null}$ males were fertile and showed no significant differences compared to controls ($sakura^{+/+}$ and $sakura^{null/+}$) (**Fig S2**).

To confirm that the observed female sterility was caused by the loss of *sakura*, we generated *sakura* rescue flies expressing Sakura-EGFP in the $sakura^{null/null}$ background ($sakura^{null/null}$; *sakura-EGFP*). Western blotting confirmed that these flies expressed Sakura-EGFP, but not endogenous Sakura (**Fig 1D**). The *sakura-EGFP* transgene fully rescued both female fertility and ovary morphology in the $sakura^{null/null}$ background (**Fig 2**). *sakura-EGFP* rescue females showed no significant fertility differences compared to controls (**Fig 2A** and **2B**), and their ovaries were normal in shape and size (**Fig 2C**). We concluded that Sakura is essential for female fertility and normal ovary morphology but dispensable for male fertility, consistent with the observation that Sakura is predominantly expressed in ovarian germline cells (**Fig 1**).

$sakura^{null/null}$ ovaries are germless and tumorous

Given the rudimentary appearance of $sakura^{null/null}$ ovaries, we questioned whether they contained germ cells. We used flies carrying *vasa-EGFP* knocked-in reporter in the $sakura^{null/null}$ background, as Vasa is a known germ cell marker. We observed that some $sakura^{null/null}$ovarioles were devoid of germ cells ("germless", cyan stars), while others retained germ cells (**Fig 3A** and **3B**). Immunostaining with HTS antibody revealed an excess number of GSC-like cells with round spectrosomes in $sakura^{null/null}$ ovarioles containing germ cells (**Fig 3C**, orange stars), indicative of a "tumorous" phenotype as previously described for mutants of other genes including *bam*, *otu*, and *sxl* (Smith and King 1966; Gans et al. 1975; Gollin and King 1981; King and Riley 1982; McKearin and Spradling 1990; Bopp et al. 1993; Eliazer et al. 2011; Jin et al. 2013; Yang et al. 2019). Additionally, we observed an excess number of cyst cells with branched fusomes that persisted throughout the ovarioles, suggesting abnormal cyst cell differentiation and division. Thus, loss of *sakura* results in both germ cell depletion and overgrowth.

Within the same ovary, some $sakura^{null/null}$ ovarioles exhibited the tumorous phenotype, while others were germless, without any spectrosome or fusome staining (**Fig 3A-3C**, cyan stars). Quantification revealed that 35% of $sakura^{null/null}$ ovarioles from 2- to 5-day-old flies were tumorous, while the remaining 65% were germless (n=74) (**Fig 3D**). In contrast, all ovarioles in control ($sakura^{+/+}$ and $sakura^{null/+}$) and *sakura-EGFP* rescue flies were normal with no tumorous or germless phenotypes observed (**Fig 3D**). Approximately 95% of $sakura^{null/null}$ ovarioles

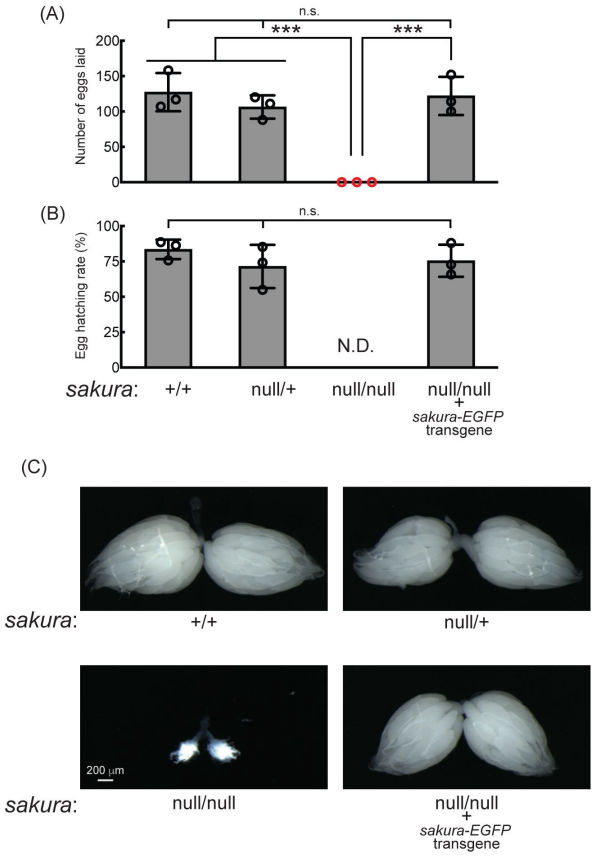

Fig 2.

sakura mutant flies are female-sterile and have rudimentary ovaries.

(A-B) Female fertility assays. (A) The number of eggs laid by test females crossed with OregonR wild-type males and (B) hatching rates of the eggs. Mean ± SD (n = 3). P-value < 0.001 (Student's t-test, unpaired, two-tailed) is indicated by ***. (C) Stereomicroscope images of dissected whole ovaries. Scale bar: 200 µm.

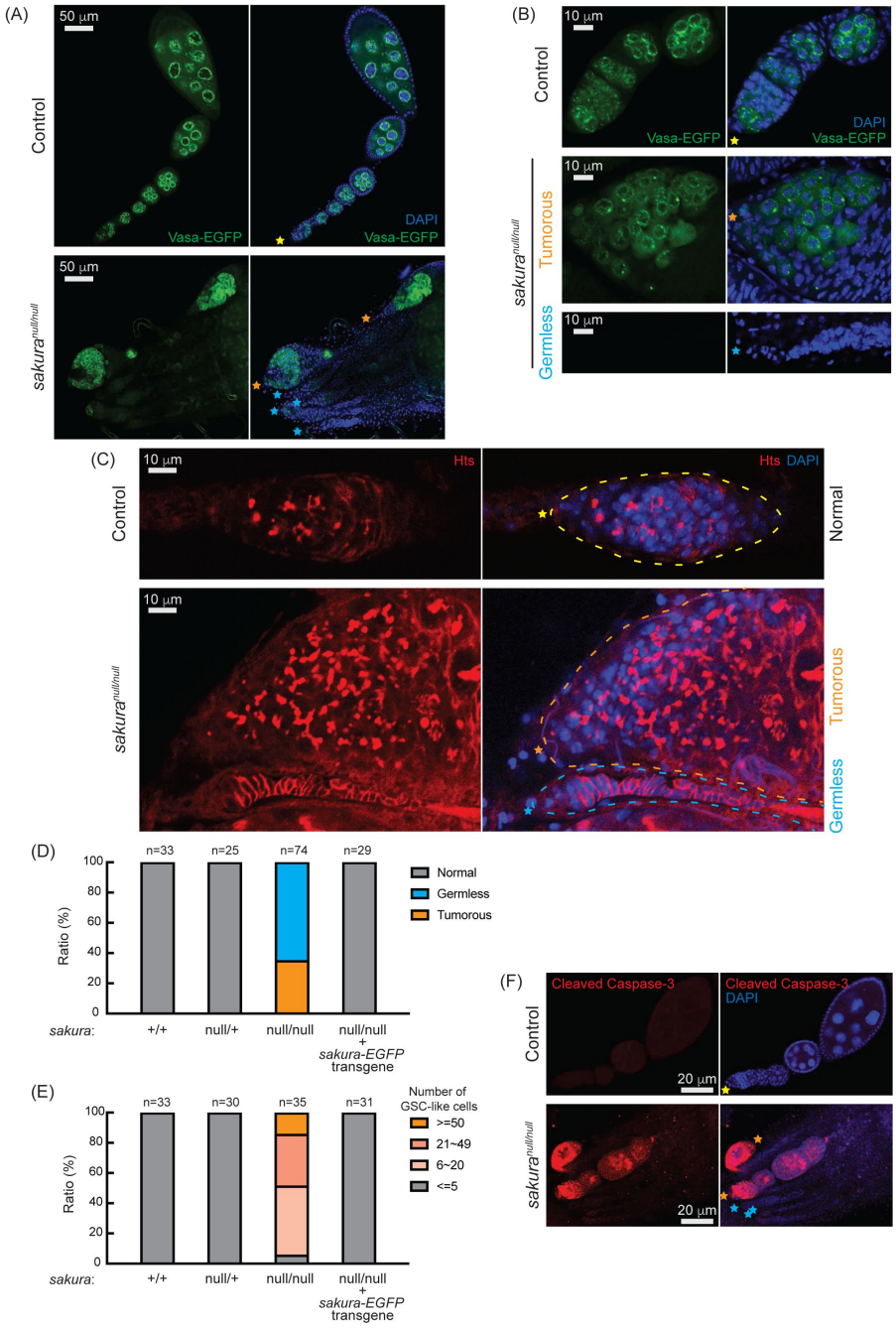

Fig 3.

sakura^{null} ovaries are germless and tumorous

(A, B) Confocal images of the ovaries from control (*sakura*$^{null/+}$) and *sakura*$^{null/null}$ expressing Vasa-EGFP. Vasa-EGFP (green) and DAPI (blue). Yellow stars indicate the anterior tip of normal ovarioles, while orange and cyan stars indicate the anterior tips of tumorous and germless ovarioles, respectively, in **Figure 1**. Higher-magnification images of the germarium regions are shown in (B). Scale bars: 10 μm for (A) and 50 μm for (B). (C) Confocal images of control (*sakura*$^{null/+}$) and *sakura*$^{null/null}$ ovaries stained with anti-Hts antibody to label spectrosomes and fusomes. Hts (red) and DAPI (blue). Yellow, orange, and cyan dotted lines mark the normal, tumorous, germless and germaria, respectively. Scale bars: 10 μm. (D) Ratio (%) of normal, germless, and tumorous ovarioles of indicated genotypes (ages 2-5 days; n=33, 25, 74, 29 respectively). (E) Quantification of GSC-like cell number per germarium in the indicated genotypes (ages 2-5 days; n = 33, 30, 35, and 31 respectively). (F) Confocal images of control (*sakura*$^{null/+}$) and *sakura*$^{null/null}$ ovaries stained with anti-cleaved Caspase-3 antibody. Cleaved caspase-3 (red) and DAPI (blue). Scale bars: 20 μm.

containing germ cells had an excess of GSC-like cells (>5) (**Fig 3E** and **Fig S4**). The mean number of GSCs or GSC-like cells in 2- to 5-day-old *sakura*$^{+/+}$, *sakura*$^{null/+}$, and *sakura-EGFP* rescue was 2.2 ± 0.6, 2.2 ± 0.6, and 2.1 ± 0.7, respectively while that for *sakura*$^{null/null}$ was 26.5 ± 17.5 (p-value <0.05).

We investigated the age-dependent effects on the tumorous and germless phenotypes by examining the ovarioles from 0-1 day old, 7-day old, and 14-day old flies. Ovarioles in control and *sakura-EGFP* rescue flies remained normal throughout this time course (**Fig S4A**). In the very young, 0-1 day old *sakura*$^{null/null}$, 78% of ovarioles were tumorous and 22% were germless. Overtime, the ratio of germless ovarioles increased while the ratio of tumorous ovarioles decreased. By 14 days old, only 5% of ovarioles were tumorous, with the remaining 95% being germless. The number of GSC-like cells in *sakura*$^{null/null}$ ovarioles was already high in 0-1 day old flies, and it decreased over time (**Fig S4B**). Tumorous ovarioles, but not germless ones, exhibited significantly higher levels of cleaved Caspase-3 staining, indicative of apoptosis, compared to controls (**Fig 3F**). These results suggest that tumorous ovarioles undergo apoptosis, and that these ovarioles eventually become germless.

Together, these results suggest that Sakura is essential for regulating the survival, proliferation, and differentiation of germline cells, including GSCs.

Loss of *sakura* results in reduced germline piRNA

In controls, Vasa-EGFP is enriched in the perinuclear structure known as the nuage within nurse cells (**Fig 3A** and **3B**), which is essential for piwi-interacting RNA (piRNA) biogenesis. In *sakura*$^{null/null}$tumorous ovarioles, Vasa-EGFP retains its perinuclear localization, indicating that *sakura* is not required for the proper localization of Vasa to the nuage.

piRNAs are produced in germline cells and somatic follicle cells and transcriptionally and post-transcriptionally silence transposon expression through sequence-complementarity (Huang et al. 2017; Yamashiro and Siomi 2018). Disruption of the piRNA pathway can result in oogenesis arrest, germ cell loss, rudimentary ovaries, and sterility. Loss of piRNAs in germ cells leads to the upregulation (desilencing) of transposons, increased DNA damage, and apoptotic cell death[31]. We investigated whether the loss of *sakura* would result in loss of piRNA and transposon upregulation. We performed high-throughput sequencing (small RNA-seq and polyA+ RNA-seq) on ovary RNA samples from *sakura*$^{+/+}$, *sakura*$^{null/+}$, *sakura*$^{null/null}$, and *sakura-EGFP* rescue (*sakura*$^{null/null}$ with *sakura-EGFP*) flies.

piRNA levels in *sakura*$^{null/null}$ ovaries were reduced compared to controls (*sakura*$^{+/+}$), while *sakura*$^{null/+}$ and *sakura-EGFP* rescue showed no such reduction (**Fig 4A**). Consistent with this, transposon RNA levels in *sakura*$^{null/null}$ ovaries were upregulated compared to *sakura*$^{+/+}$, while *sakura*$^{null/+}$ and *sakura-EGFP* rescue showed no such upregulation (**Fig 4B**). Given that Sakura is specifically expressed in germline cells, but not in somatic cells (**Fig 1E** and **1F**), we hypothesized that loss of *sakura* interrupts the piRNA pathway in germ cells, leading to the desilencing of germline transposons. A well-characterized germline transposon in *Drosophila* is *Burdock* (Donertas et al. 2013; Handler et al. 2013). We found that *Burdock* piRNA levels were significantly lower in *sakura*$^{null/null}$ compared to controls and rescue flies (**Fig 4C**).

We employed the *Burdock* sensor, a transposon reporter tool to monitor germline piRNA activity (Handler et al. 2013). The reporter expresses nuclear GFP and β-gal under the control of the *nanos* promoter for germline expression, with a target sequence for *Burdock* piRNAs in the 3' UTR (**Fig 4D**). Using a *sakura* RNAi line driven by *UAS-Dcr2* and *NGT-Gal4* to knock down *sakura* specifically in the germline, we observed that GFP and β-gal expression were highly elevated in *sakura* knockdown germlines compared to control RNAi (*y*^{RNAi}) knockdowns (**Fig 4D**). This

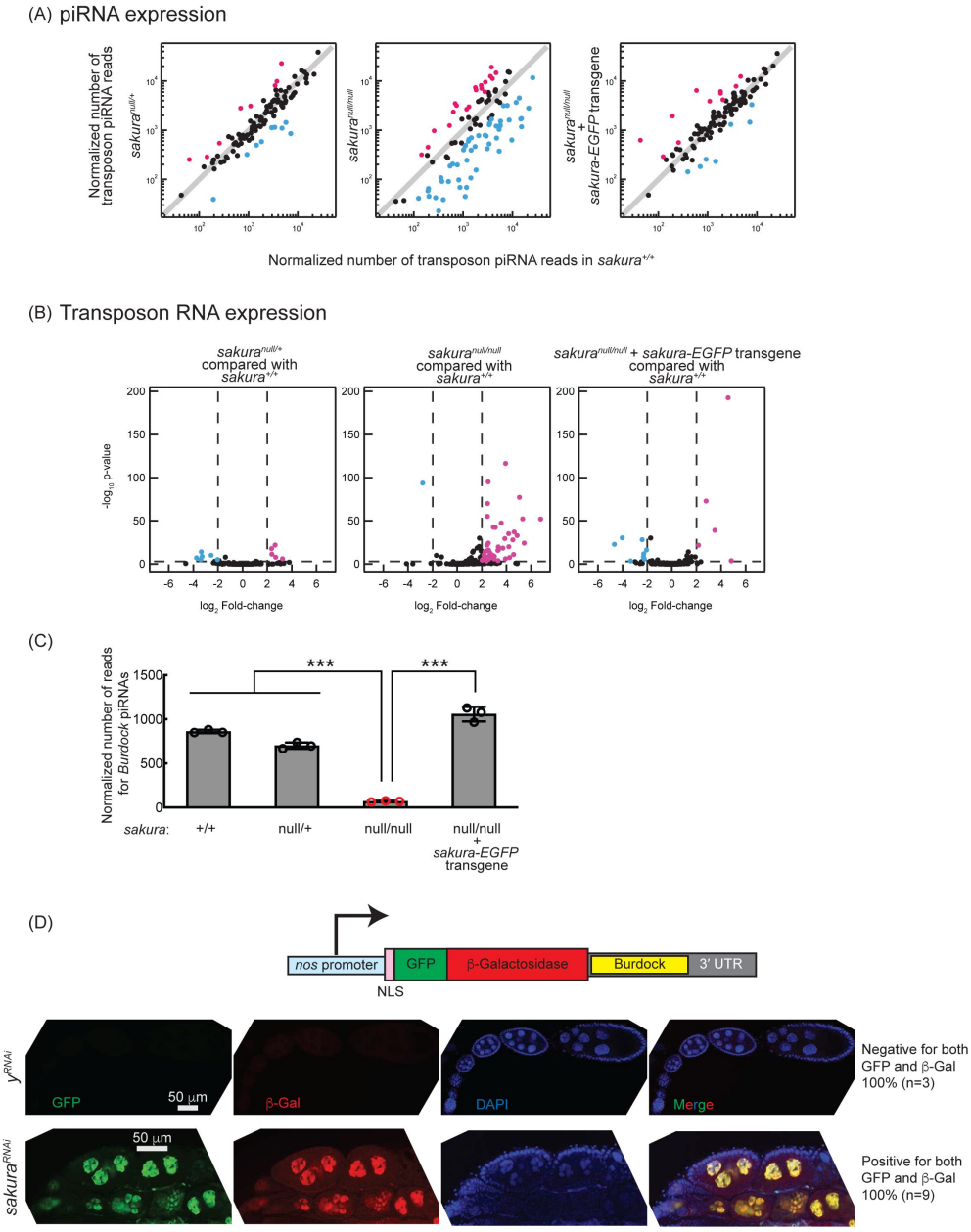

Fig 4.

Loss of *sakura* results in lower piRNA levels and loss of piRNA-mediated transposon silencing

(A) Scatter plots of normalized number of transposon piRNA reads from small RNA-seq of indicated genotypes compared with *sakura*$^{+/+}$. Means of three biological replicates are plotted. Downregulated (fold-change < 0.5) and upregulated (fold-change > 2) transposon piRNAs are shown in cyan and magenta, respectively. (B) Volcano plots of transposon RNAs from RNA-seq of indicated genotypes compared with *sakura*$^{+/+}$. Three biological replicates per genotype were analyzed. Downregulated (adjusted p-value < 0.001 and $\log_2$(fold-change) < -2) and upregulated (adjusted p-value < 0.001 and $\log_2$(fold-change) > 2) transposons are shown in cyan and magenta, respectively. (C) Normalized number of reads for *Burdock* piRNAs from small RNA-seq. Mean ± SD (n = 3.) P-value < 0.001 (Student's t-test, unpaired, two-tailed) is indicated by ***. (D) The *Burdock* sensor harbors a *nanos* promoter, a nuclear localization signal (NLS) appended to GFP and β-gal coding sequences, and a target sequence for *Burdock* piRNAs in the 3'UTR. Confocal images of ovaries from control (*y*^{RNAi}) and *sakura*^{RNAi} flies harboring the Burdock sensor, where RNAi knockdown was specifically driven in the female germline with *UAS-Dcr2* and *NGT-Gal4*. GFP (green), β-gal (red), and DAPI (blue). Scale bars: 50 μm. Three out of 3 tested control samples were negative for both GFP and β-gal, while 9 out of 9 tested *sakura*^{RNAi} samples were positive for both markers.

confirmed that loss of *sakura* leads to a loss of piRNA-mediated transposon silencing in the germline, suggesting that Sakura is essential for proper piRNA levels and piRNA-based transposon silencing in the germline.

Sex-specific *sxl* mRNA alternative splicing is dysregulated in *sakura*$^{null/null}$ ovaries

Sxl is a master regulator of sex determination in *Drosophila* (Penalva and Sanchez 2003; Salz and Erickson 2010; Grmai et al. 2022). Sex-specific alternative splicing of *sxl* transcripts produces distinct mRNA isoforms: the female-specific and male-specific mRNA isoforms in respective sex and only the female-specific mRNA isoform encodes the functional Sxl protein, whereas the male-specific isoform does not. In the female germline, loss of Sxl function or disruption of female-specific *sxl* splicing leads to developmental defects, including germline tumors and sterility. Notably, several mutants with tumorous ovariole phenotypes—including *otu* mutants—exhibit aberrant *sxl* mRNA splicing, resulting in the expression of the male-specific isoform in ovaries and defects in germ cell sexual identity (Bopp et al. 1993; Pauli et al. 1993).

We examined *sxl* splicing in *sakura* mutants. As expected, ovaries from control and *sakura-EGFP* rescue flies expressed exclusively the female-specific *sxl* mRNA isoform and testes from control flies expressed only the male-specific isoform (**Fig S5**). In contrast, *sakura*$^{null/null}$ovaries exhibited the male-specific isoform and a reduced level of the female-specific isoform. These results indicate that female-specific *sxl* alternative splicing is disrupted in the absence of *sakura*.

sakura is important for oogenesis in germline cells beyond GSCs and germline cysts

Both *sakura*$^{null/null}$ and *sakura* germline RNAi knockdown driven by *UAS-Dcr-2* and *NGT-Gal4*, which initiates RNAi in germline from GSCs, resulted in rudimentary ovaries (**Fig 2C** and **5A**). These ovaries lacked later-stage germline cells and egg chambers, making it difficult to assess the role of Sakura beyond the germarium. However, because Sakura-EGFP expression is not limited to GSCs and germline cysts (**Fig 1E** and **1F**), we speculated that Sakura might function in later-stage germline cells as well.

To explore this possibility, we used *TOsk-Gal4* (a combination of *osk-Gal4* and *αTub67C-Gal4*) to drive *sakura* RNAi knockdown in germline cells after the germline cyst stage (from germarium region 2b onward. **Fig 1A**), sparing GSCs and germline cysts (ElMaghraby et al. 2022). Unlike *NGT-Gal4*, *TOsk-Gal4*-driven *sakura* RNAi knockdown did not drastically affect ovary morphology (**Fig 5A**), allowing us to study the effects of *sakura* loss in egg chambers. We confirmed *sakura* RNAi (*sakura RNAi #1* and *#2*) knockdown efficiency by Western blot, showing effective depletion of Sakura in ovaries from both *NGT-Gal4* and *TOsk-Gal4*-driven RNAi lines (**Fig 5B**).

Interestingly, *TOsk-Gal4*-driven *sakura* RNAi knockdown severely reduced the numbers of eggs laid (**Fig 5C**) and stage 14 oocytes in ovaries compared to control RNAi (y^{RNAi}) (**Fig 5D**), suggesting that *sakura* is important for oogenesis beyond the germline cyst stage. Additionally, we observed mislocalized and dispersed Oo18 RNA-binding protein (Orb), a marker for oocyte identity, in *TOsk-Gal4*-driven *sakura* RNAi ovaries beginning around stage 6 of oogenesis (**Fig 5E**). In controls, Orb was enriched and properly localized to the posterior end of stage ~6-8 egg chambers (**Fig 5E**, yellow arrows). In *sakura*^{RNAi} ovaries, although Orb localization appeared normal at stage ~6 (yellow arrow), mislocalization was evident by stage ~8 (magenta arrow), and signs of cytoskeletal disorganization were apparent in later-stage egg chambers (white arrowheads). Phalloidin staining to visualize F-actin further supported cytoskeletal defects in *sakura*^{RNAi} later-stage egg chambers (**Fig S6**).

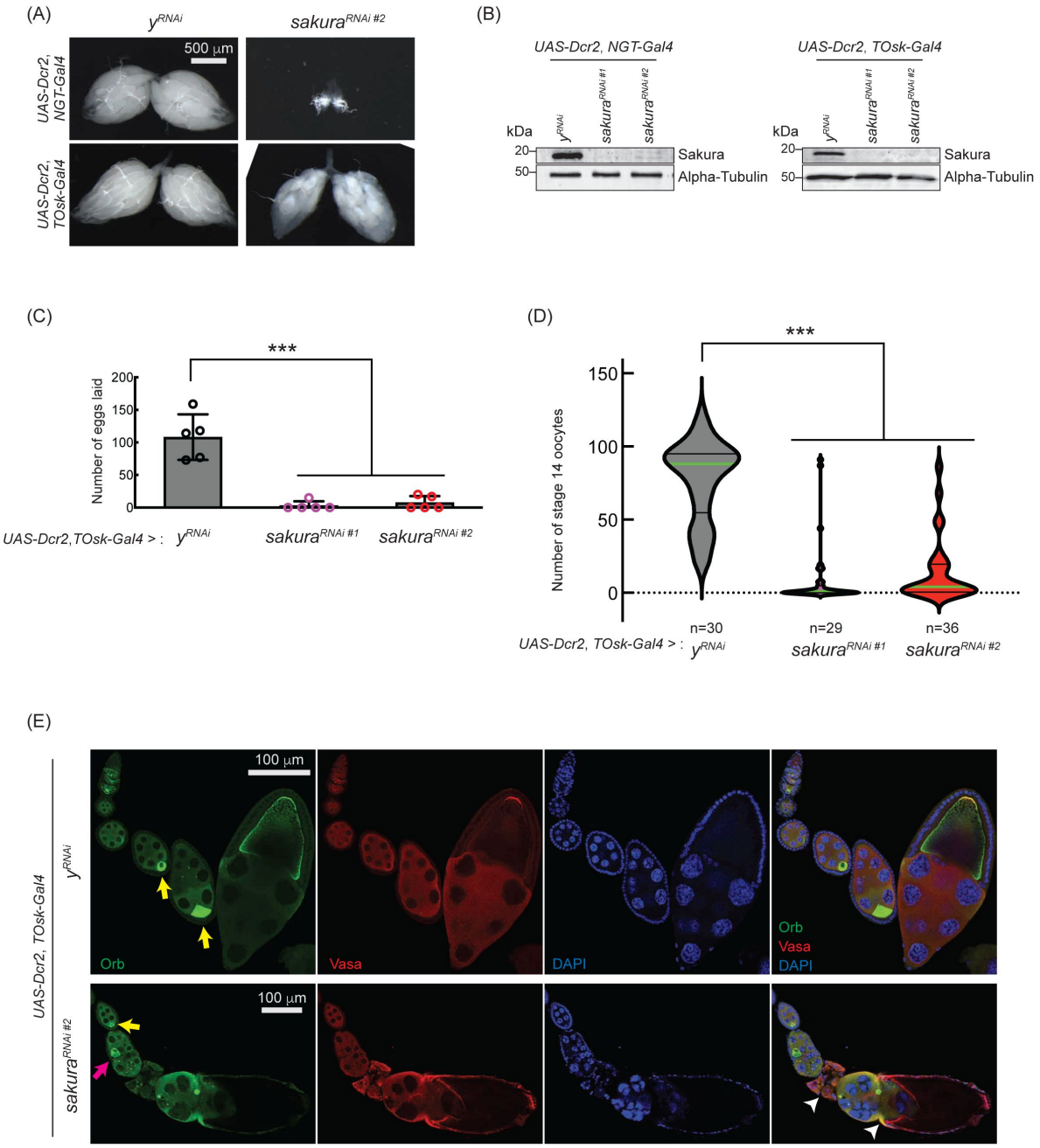

Fig 5.

sakura is important for oogenesis in later-stage egg chambers

(A) Stereomicroscope images of dissected whole ovaries. Scale bar: 500 µm. (B) Western blot of dissected Ovary lysates. *sakura*$^{RNAi\ \#1}$ and *sakura*$^{RNAi\ \#2}$ are two independent RNAi lines. (C) Number of eggs laid by *sakura* RNAi knockdown driven by *UAS-Dcr2* and *TOsk-Gal4*. Mean ± SD (n = 5). P-value < 0.001 (Student's t-test, unpaired, two-tailed) is indicated by ***. (D) Number of stage 14 oocytes in ovaries of *sakura* RNAi knockdown flies driven by *UAS-Dcr2* and *TOsk-Gal4*. The numbers of stage 14 oocytes per fly (per a pair of ovaries) are shown. n is the numbers of flies examined. P-value < 0.001 (Student's t-test, unpaired, two-tailed) is indicated by ***. (E) Confocal images of the ovaries from *sakura* RNAi knockdown flies driven by *UAS-Dcr2* and *TOsk-Gal4*, stained with anti-Orb and anti-Vasa antibodies. Orb (green), Vasa (red), and DAPI (blue). Yellow arrows label the normal enrichment of Orb in the developing oocytes. Magenta arrow labels mislocalized developing oocyte. White arrowheads label egg chambers with cytoskeletal disorganization. Scale bars: 100 µm. In A-E, *y-RNAi* was used as a control.

These defects likely contribute to the impaired production of stage 14 oocytes and eggs in *sakura*^{RNAi} flies (**Fig 5C** and **5D**). We conclude that Sakura plays an essential role in oogenesis beyond the early germline stages. For all subsequent *sakura* RNAi experiments, we used the *sakura RNAi* #2 line.

Sakura is required intrinsically for GSC establishment, maintenance, and differentiation

To investigate whether *sakura* functions autonomously in the germline, we performed mosaic analysis using the FLP-FRT system with heat shock promoter-driven FLP (*hs-flp*) (Xu and Rubin 1993; Rubin and Huynh 2015). First, to assesse its role in GSC establishment, we induced *sakura*^{null} clones in primordial germ cells (PGCs) by applying heat shock before the early third instar larval stage and tracked their development into adult GSCs, following a previously established protocol (Yang et al. 2007). In control adult flies (*FRT82B*),12.3% (20/163) of GSCs were marked, wheras only 1.9% (4/213) were marked in *sakura*^{null}mutants (*FRT82B*, *sakura*^{null}) (p-value = 4.8 * 10^{-11}, chi-square test), indicating that *sakura* is autonomously required for GSC establishment.

Next, we assessed GSC maintenance using the same system by generating *sakura*^{null} GSC clones in adult flies and measuring clone loss over time, as described previously (Xie and Spradling 1998; Yang et al. 2007). Four days after clone induction, 27.8% of GSCs were marked in controls (*FRT82B*) and 22.1% in *sakura*^{null} (*FRT82B*, *sakura*^{null}), which we defined as initial levels (**Fig 6A**). In controls, the percentage of marked GSCs declined to 25.8% on day 7 and and 16.8% on 14, resulting in a 39.4% loss rate over 10 days (from day 4 to day 14). In contrast, the proportion of marked *sakura*^{null} GSC clones dropped more sharply—to 16.3% on day 7 and and 5.4% on day 14—yielding a higher loss rate of 75.6% over 10 days. These results demonstrate that *sakura* is intrinsically important for GSC maintenance.

We further tested whether *sakura* is intrinsically required for GSC differentiation, we quantified the number of marked (GFP-negative) and unmarked (GFP-positive) GSC-like cells (germline cells with a round spectrosome) in the germaria containing marked GSC clones at days 4, 7, and 14 post-induction (**Fig 6B**). We found that marked *sakura*^{null} GSC-like cells were significantly more numerous than marked control GSC-like cells at all time points (**Fig 6C**). The number of marked *sakura*^{null}GSC-like cells increased over the 10-day period, while the number of marked control cells did not (**Fig 6C**). In contrast, unmarked GSC-like cells in germaria containing *sakura*^{null}GSC clones did not differ significantly in number compared with those in germaria containing marked control GSC clones, and the number did not increase over time (**Fig S8**).

These results demonstrate that *sakura* is intrinsically important in germline cells, including GSCs, to regulate proper division and differentiation. In the absence of intrinsic *sakura*, germline cells become tumorous and undergo uncontrolled proliferation. Taken together, we conclude that *sakura* is required intrinsically for GSC establishment, maintenance, and differentiation.

Loss of *sakura* inhibits Dpp/BMP signaling

The Dpp/BMP signaling pathway plays a central role in regulating *bam* expression and GSC self-renewal and differentiation (**Fig 7A**) (Kirilly and Xie 2007; Hayashi et al. 2020). We hypothesized that the germless and tumorous phenotypes observed in *sakura* loss-of-function ovaries could be due to Dpp/BMP signaling misregulation. To test this, we knocked down *sakura* in the germline driven by *UAS-Dcr2* and *NGT-Gal4* in the presence of *bam-GFP* reporter (Chen and McKearin 2003b). In controls (*y*^{RNAi}), Bam-GFP expression was restricted to 8-cell cysts and disappeared in 16-cell cysts and onward (**Fig 7B**). In contrast, *sakura* knockdowns ovaries showed persistent Bam-GFP expression throughout the germarium including the GSC niche region (**Fig 7B**).

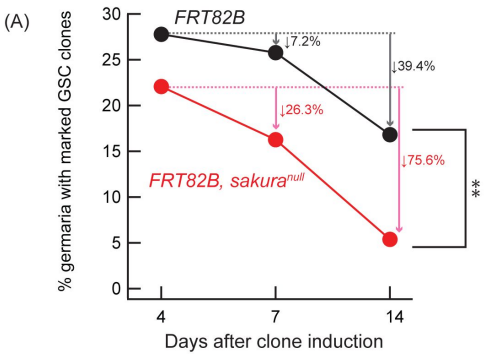

Genotype	Days after stopping heat shock	% marked GSCs	Relative % marked GSCs	Total number of germaria examined
hs-flp/w; +; FRT82B, ubi-GFP / FRT82B (control)	4	27.8	100	108
	7	25.8	92.8	97
	14	16.8	60.6	101
hs-flp/w; +; FRT82B, ubi-GFP / FRT82B, sakura^null	4	22.1	100	77
	7	16.3	73.7	86
	14	5.4	24.4	167

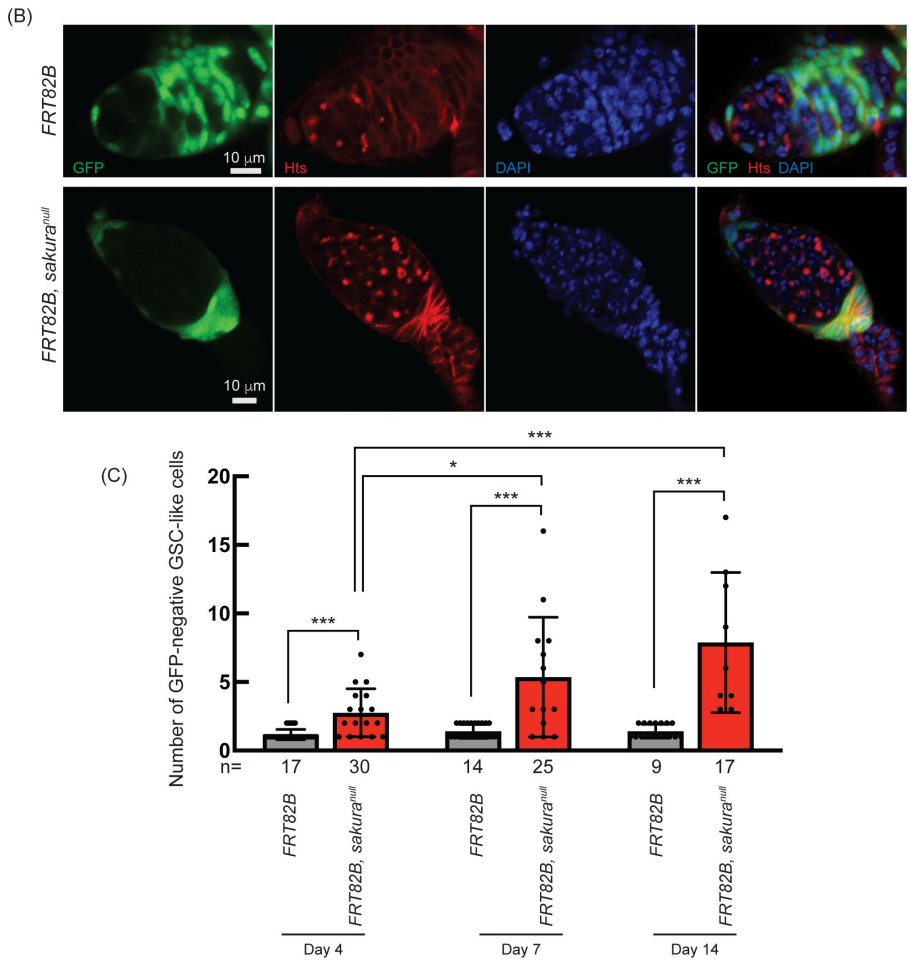

Fig 6.

Germline clonal analysis of *sakura^null*

(A) Percentage of germaria with marked GSC clones indicated by the absence of GFP at 4, 7, and 14 days after clone induction at the adult stage. Arrows indicate the percent decrease of marked GSC clones compared to day 4. The genotype, actual percentage, and total number of germaria examined are shown in the adjacent table. P-value < 0.01 (Chi-squared test) is indicated by **. (B) Confocal images of Germ cell clones. *sakura^null* and control clones were marked by the absence of GFP. GFP (green), Hts (red), and DAPI (blue). Scale bars: 10 μm. (C) Number of marked (GFP-negative) GSC-like cells in germaria with marked GSCs of the indicated genotypes at 4, 7, and 14 days after clone induction. GSC-like cells containing round spectrosome were identified through immunostaining with anti-Hts antibody. P-value < 0.05 and <0.001 (Student's t-test, unpaired, two-tailed) is indicated by * and ***, respectively.

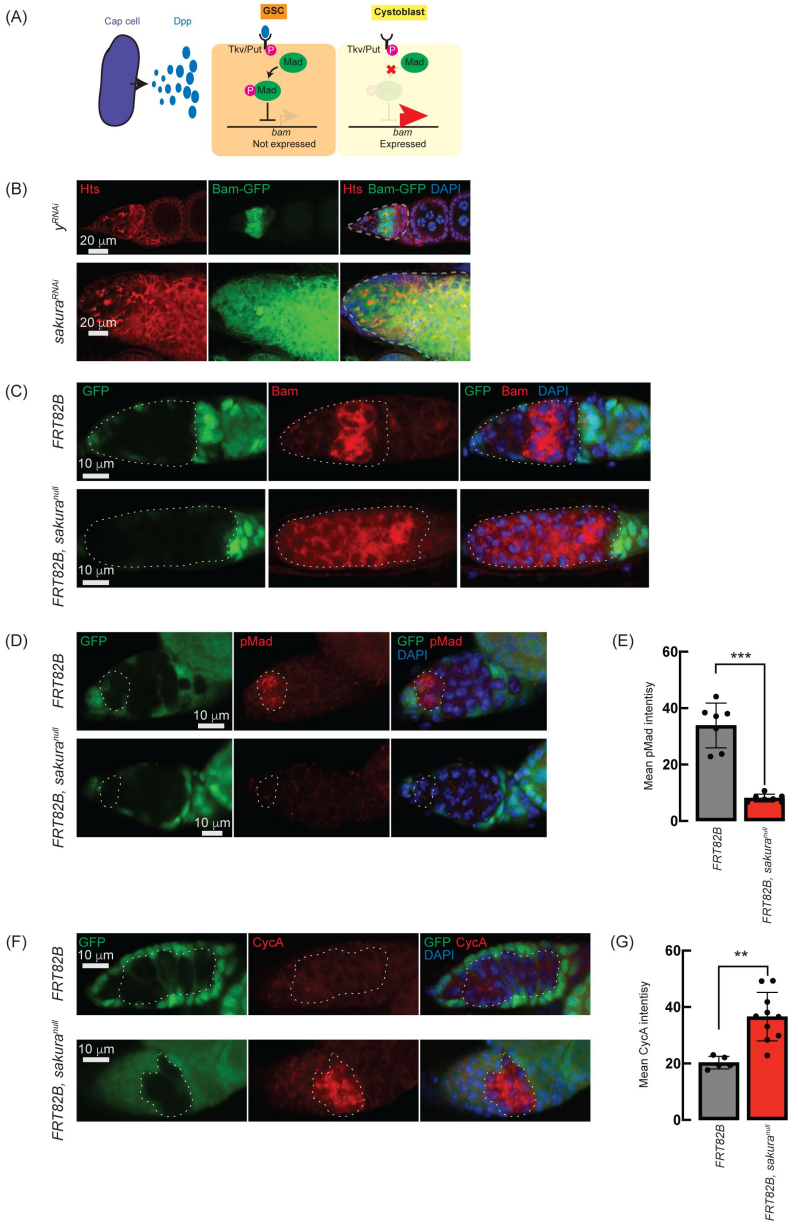

Fig 7.

Loss of *sakura* inhibits Dpp/BMP signaling

(A) Schematic illustration of bam expression regulation. Cap cells secrete diffusible Decapentaplegic (Dpp), which is received by its receptor, a heterodimer of Thick vein (Tkv) and Punt (Put), in GSCs. The activated Dpp signaling eventually phosphorylates Mother-against-dpp (Mad). The phosphorylated Mad (pMad) represses the transcription of *bag-of-marbles* (*bam*). The repression of *bam* in GSCs is crucial for maintaining their stemness. Cystoblasts do not receive Dpp, and Bam expression is crucial for promoting cystoblast differentiation from GSCs. (B) Confocal images of ovaries from control (y^{RNAi}) and $sakura^{RNAi}$ flies harboring the *bam-GFP* reporter, where RNAi knockdown was specifically driven in the female germline with *UAS-Dcr2* and *NGT-Gal4*. Bam-GFP (green), Hts (red), and DAPI (blue). Germarium are outlined by dotted line. Scale bars: 20 μm. (C, D) Confocal images of germaria with germline clones of $sakura^{null}$stained with (C) anti-Bam antibody and (D) anti-pMad antibody. GFP (green), Bam or pMad (red), and DAPI (blue). Scale bars: 10 μm. (E) Mean pMad intensity in the germline clones of the indicated genotypes. Mean ± SD (n = 7). P-value < 0.001 (Student's t-test, unpaired, two-tailed) is indicated by *** (F) Confocal images of germaria with germline clones of $sakura^{null}$ stained with anti-CycA antibody. GFP (green), CycA (red), and DAPI (blue). Scale bars: 10 μm. (G) Mean CycA intensity in the germline clones of the indicated genotypes. Mean ± SD (n = 5 and 10 for *FRT82B* and *FRT82B,* $sakura^{null}$ respectively). P-value < 0.01 (Student's t-test, unpaired, two-tailed) is indicated by **. In C, D, and F, clones were marked with the absence of GFP.

To further confirm this finding, we used the FLP-FRT system to induce *sakura*^{null} clones in germaria and performed immunostaining with anti-Bam antibody. In control clones (*FRT82B*), Bam expression was observed exclusively in 8-cell cysts. However, in all *sakura*^{null} clones (*FRT82B*, *sakura*^{null}), Bam was aberrantly expressed throughout the germarium, including in GSCs (**Fig 7C**). These results suggest that in the absence of *sakura*, Bam expression is no longer repressed by Dpp/BMP signaling in the GSC niche, leading to GSC loss, and is no longer shut off after the 16-cell cyst stage.

In GSCs, pMad translocates into the nucleus to repress Bam expression (**Fig 7A**) (Kai and Spradling 2003; Song et al. 2004). We stained ovaries with anti-pMad antibodies and found that pMad intensity was significantly reduced in *sakura*^{null} GSC clones compared to control GSCs (**Fig 7D and E**). This indicates that the dysregulated Bam expression observed in *sakura*^{null} was due to reduced pMad levels in GSCs.

Previous studies have shown that ectopic expression of a stable form of CycA leads to germ cell loss (Chen et al. 2009). This germ cell loss phenotype is also observed upon ectopic *bam* expression in GSCs (Xie and Spradling 1998; Chen and McKearin 2003a; Xia et al. 2010). It was reported that Bam associates with Ovarian tumor (Otu) to promote deubiquitination and stabilization of CycA (Ji et al. 2017). Since we observed derepressed *bam* expression in *sakura*^{null}cells, we investigated whether CycA levels were affected. Staining ovaries with anti-CycA antibodies revealed higher CycA intensity in *sakura*^{null} clones compared to neighboring wild-type cells in the same germarium (*FRT82B*, *sakura*^{null}) and control clones in control germarium (*FRT82B*) (**Fig 7F**). *sakura*^{null} clones exhibited significantly higher mean CycA intensity compared to control clones (**Fig 7G**). The elevated CycA levels in *sakura*^{null} clones likely results from Bam misexpression and Bam-mediated stabilization.

To determine whether *bam* misexpression occurs in egg chambers in *sakura* knockdown conditions, we examined *bam* expression in TOsk-Gal4-driven *sakura* RNAi flies. Bam was appropriately restricted to 8-cell cysts in germaria and not misexpressed in egg chambers compared to yRNAi controls (**Fig. S8**, cyan arrowheads). Thus, *sakura* is specifically required in GSCs and cyst cells to regulate *bam* expression.

We also examined DE-Cadherin (DE-Cad), which plays a role in oocyte positioning within the egg chamber (Godt and Tepass 1998). DE-Cad level and localization appeared normal in both control and *sakura* RNAi ovaries through approximately stage 8. However, later-stage egg chambers in *sakura* RNAi flies displayed structural disorganization (**Fig. S8**, white arrowheads), consistent with defects observed in **Fig. 5E** and **Fig. S6**.

Attempts to rescue *sakura* loss-of-function ovariole phenotypes

To determine whether the phenotypes caused by *sakura* loss-of-function could be rescued, we first performed genetic interaction experiments by knocking down either *bam* or *cycA* in the germline. As expected, germline-specific *bam* RNAi driven by *UAS-Dcr2* and *NGT-Gal4* resulted in 100% tumorous ovarioles, while *cycA* RNAi produced 100% normal ovarioles in 2–5-day-old flies (**Fig. S9A**). Double knockdown of *sakura* and *bam* reduced the proportion of germless ovarioles and increased the proportion of tumorous ovarioles compared to *sakura* RNAi alone or the double knockdown of *sakura* and control *w* RNAi. However, no normal ovarioles were observed (**Fig. S9A**). *sakura* and *cycA* double knockdown had no effect on the phenotype distribution, suggesting that the germless phenotype in *sakura* mutants is partially attributable to ectopic *bam* expression but not to *cycA* misregulation.

The number of GSC-like cells was increased in *sakura* and *bam* double knockdowns compared to *sakura* RNAi or *sakura* and *w* double RNAi, whereas *sakura* and *cycA* knockdown did not alter GSC-like cell numbers (**Fig. S9B**), further supporting a genetic interaction between *sakura* and *bam*.

Next, we tested whether the *sakura* loss-of-function phenotypes could be rescued by overexpressing components of the Dpp/BMP signaling pathway. Germline expression of *UASp-Mad-GFP* driven by *nos-Gal4-VP16* in both $sakura^{null/+}$ controls and $sakura^{null/null}$ did not alter the proportions of ovariole phenotypes (**Fig S10A**) or the number of GSC-like cells (**Fig S10B**). Thus, transgenic overexpression of Mad did not rescue the *sakura* mutant phenotypes.

We then tested whether overexpression of a constitutively active form of the Dpp receptor Thickveins (Tkv.Q253D) (Casanueva and Ferguson 2004) could rescue the phenotypes. Expression of *UASp-tkv.Q253D* in the germline using a *NGT-Gal4* in a control (y^{RNAi}) background resulted in 100% tumorous ovarioles, as expected (**Fig. S11A**). When co-expressed with *sakura* RNAi, Tkv.Q253D increased the proportion of tumorous ovarioles and decreased the proportion of germless ovarioles relative to $sakura^{RNAi}$ alone but did not restore normal ovarioles. The number of GSC-like cells was also increased by Tkv.Q253D expression in $sakura^{RNAi}$ (**Fig S11B**), indicating partial phenotypic modulation via BMP pathway activation.

Sakura binds Otu

To explore the molecular function of Sakura in oogenesis, we aimed to identify Sakura-interacting proteins. We conducted a co-immunoprecipitation experiment using anti-GFP magnetic beads on the ovary lysates of flies expressing Sakura-EGFP, followed by mass spectrometry to identify co-immunoprecipitated proteins. Ovary lysates from flies without the *sakura-EGFP* transgene (*w1118*) served as negative controls. Mass spectrometric analysis revealed several proteins with peptide signals present in all three biological replicates of the Sakura-EGFP samples without any signals in any of the three biological replicates of the negative control (**Table 1**). Among these, the most promising candidate, exhibiting the highest unique peptide signal in each of three replicates of the Sakura-EGFP samples was Otu.

To confirm this finding, we generated a polyclonal anti-Otu antibody and validated it by Western blots using ovary lysates from the hypomorphic otu^{14} mutant (**Fig S12A**) (King et al. 1986; Storto and King 1987; Steinhauer and Kalfayan 1992a; Pauli et al. 1993). Using this antibody, we detected endogenous Otu protein in the Sakura-EGFP immunoprecipitants from ovaries of 3–7-day-old flies, but not in the negative control (**Fig 8A**), validating the mass spectrometry results. Next, using wild-type (without Sakura-EGFP) ovary lysates from 3–7-day old-flies, we immunoprecipitated endogenous Sakura with anti-Sakura antibody and detected endogenous Otu in the immunoprecipitant by Western blot (**Fig 8B**), demonstrating that endogenous Sakura interacts with endogenous Otu. Furthermore, we found that ectopically expressed Flag-tagged Otu co-immunoprecipitated with ectopically expressed HA-tagged Sakura in S2 cells (**Fig 8C**).

The *otu* gene encodes two annotated protein isoforms, a predominant 98 kDa isoform and a less abundant 104 kDa isoform generated by alternative splicing (Steinhauer and Kalfayan 1992b). The 98 kDa isoform lacks the Tudor domain, which is encoded by an alternatively spliced 126-nucleotide exon (**Fig 9B**. Otu(ΔTudor)) (Van Buskirk and Schupbach 2002). Previous studies have shown that the 104 kDa Otu isoform is more abundant in predifferentiated germline cells and is sufficient to carry all known Otu functions, whereas the 98 kDa Otu isoform becomes prominent during later stages of oogenesis and is implicated in nurse cell regression and oocyte maturation (Sass et al. 1995). Consistent with these findings, we observed that ovaries from very young (2–5 hour old) flies—containing only germaria and previtellogenic egg chambers—predominantly expressed the 104 kDa isoform (**Fig S12B**). In contrast, ovaries from 3–7 day old flies—containing all 14 stages of oogenesis—predominantly expressed the 98 kDa isoform. Importantly, both the 104 kDa and 98 kDa isoforms co-immunoprecipitated with endogenous Sakura using anti-Sakura antibody, demonstrating that Sakura interacts with both isoforms of Otu and that the Tudor domain is not required for this interaction (**Fig. S12B**).

Table 1.

Number of unique peptide counts detected by mass-spec.

Proteins with peptide signals present in all three biological replicates of the Sakura-EGFP samples without any signals in any of the three biological replicates of the negative control are shown.

Identified protein name	Gene ID	Unique peptide counts					
		Sakura-EGFP samples			w1118 samples (negative control)		
		Replicate 1	Replicate 2	Replicate 3	Replicate 1	Replicate 2	Replicate 3
Ovarian tumor	CG12743	44	38	18	0	0	0
Uncharacterized protein Dmel_CG4679	CG4679	17	8	2	0	0	0
Uncharacterized protein Dmel_CG14997	CG14997	17	7	2	0	0	0
Mitochondrial ribosomal protein S22	CG12261	14	6	1	0	0	0
Tudor	CG9450	15	1	1	0	0	0
Mitochondrial ribosomal protein S5	CG40049	10	4	1	0	0	0
HECT and RLD domain containing protein 2	CG11734	4	9	1	0	0	0
Mitochondrial ribosomal protein S10	CG4247	5	3	1	0	0	0
Mitochondrial ribosomal protein S31	CG5904	3	1	1	0	0	0
Uncharacterized protein Dmel_CG1316	CG1316	2	1	1	0	0	0

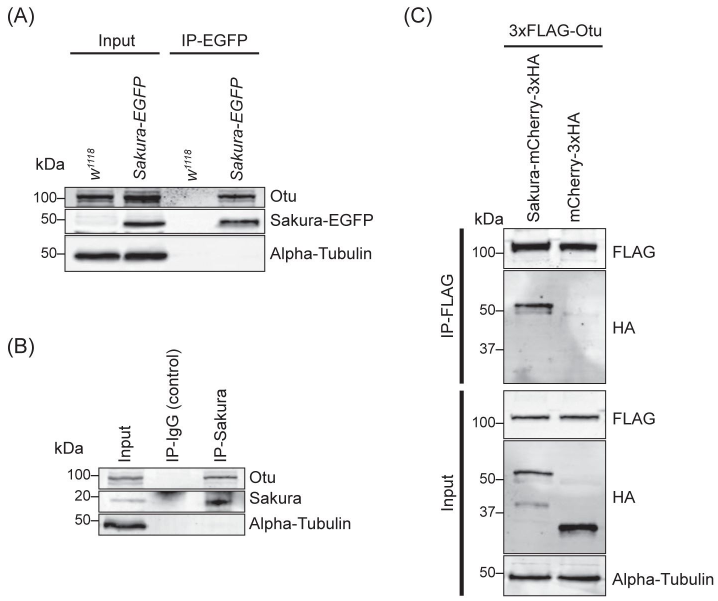

Fig 8.

Sakura interacts with Otu.

(A) Co-immunoprecipitation using anti-GFP magnetic beads followed by Western blotting. Ovary lysates expressing Sakura-EGFP in *sakura*$^{+/+}$ background and those from *w*^{1118} negative control were tested. (B) Co-immunoprecipitation using beads bound with rabbit anti-Sakura followed by Western blotting. Ovary lysates from *w*^{1118} flies were used. Rabbit IgG was used as control IP. (C) Co-immunoprecipitation using beads bound with anti-FLAG antibody followed by Western blotting. S2 cell lysates expressing 3xFLAG-Otu and Sakura-mCherry-3xHA or mCherry-3xHA (negative control) were used.

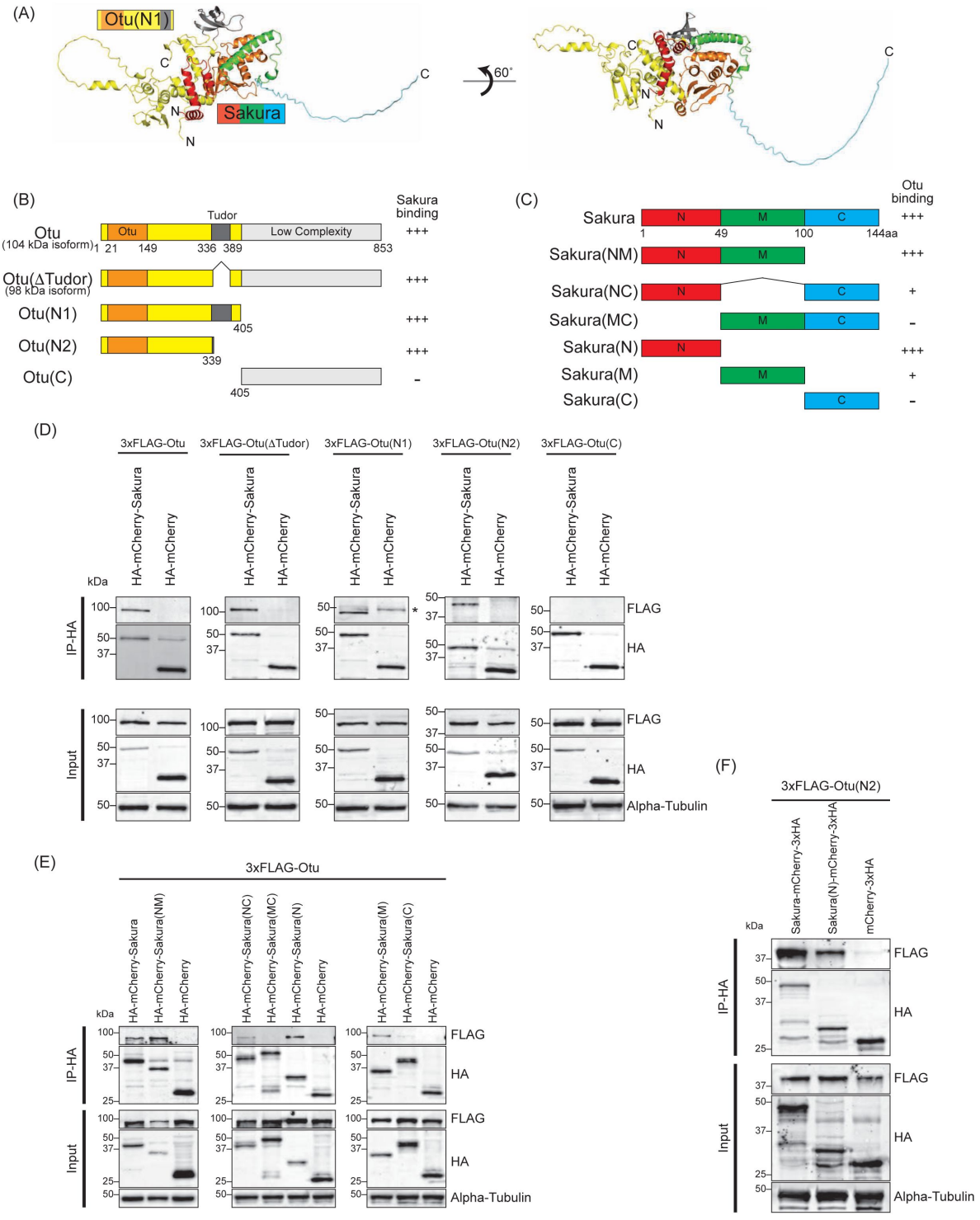

Fig 9.

N-terminal regions of Sakura and Otu are important for interaction.

(A) Predicted structure of the Sakura and Otu protein complex made by AlphaFold. Full-length Sakura and N-terminal Otu fragment (N1. 1-405aa) were used for prediction. (B) Full-length Otu and Otu fragments tested in co-immunoprecipitation assays. The binding assay results from (D) is summarized. (C) Full-length Sakura and Sakura fragments tested in co-immunoprecipitation assays (N: N-terminal, M: middle, C: C-terminal). The binding assay results from (E) is summarized. (D, E, F) Co-immunoprecipitation using anti-HA magnetic beads followed by Western blotting. S2 cell lysates expressing HA-tagged mCherry were used as negative controls.

Next, we sought to identify which regions of Sakura and Otu are important for their interaction. We predicted the structure of the Sakura-Otu protein complex using AlphaFold (Jumper et al. 2021; Yang et al. 2023). AlphaFold suggested that the N-terminal region of Sakura (1-49aa) and the N-terminal region of Otu (1-405aa) are highly likely to form interactions, while the C-terminal region of Sakura (100-144aa) does not interact with Otu (**Fig 9A-C**). The Tudor domain of Otu is not directly involved in this interaction, consistent with our findings (**Fig S12B**). To experimentally validate the predictions made by AlphaFold, we generated a series of truncated Otu fragments, including Otu(ΔTudor) (1-336, 389-853aa, corresponding to the endogenous 98 kDa isoform), Otu(N1) (1-405aa), Otu(N2) (1-339aa), and Otu(C) (405-853aa) (**Fig 9B**). We then performed co-immunoprecipitation assays to test which fragments could interact with full-length Sakura. All fragments except Otu(C) were associated with full-length Sakura protein in S2 cells (**Fig 9D**), demonstrating that the C-terminal low-complexity region of Otu is dispensable for the interaction. This assay also showed that the Tudor domain is not critical and the N-terminal fragment (1-339aa) of Otu is sufficient for interaction with Sakura. These findings align well with the predictions made by AlphaFold.

Subsequently, we created several truncated Sakura fragments and conducted co-immunoprecipitation assays in S2 cells to determine which Sakura fragments can interact with full-length Otu. The fragments generated included Sakura(NM) (1-100aa), Sakura(NC) (1-49, 100-144aa), Sakura(MC) (49-144aa), Sakura(N) (1-49aa), Sakura(M) (49-100aa), and Sakura(C) (100-144aa) (**Fig 9C**). We found that Sakura(NM), Sakura(NC), Sakura(N), and Sakura(M) were associated with Otu (**Fig 9E**). Compared to Sakura(NM) and Sakura(N), the interaction of Sakura(M) with Otu is relatively weaker, as indicated by a fainter band in the Western blot (**Fig 9E**). Sakura-NC exhibited a weak interaction with Otu, while Sakura(MC) and Sakura(C) showed no interaction (**Fig 9E**). These assays demonstrated that the N-terminal region (1-49aa) of Sakura is sufficient for interaction with Otu. Moreover, the results suggest that the C-terminal region of Sakura (100-144aa) does not interact with Otu and that adjoining it with the N-terminal (1-49aa) or the middle (M) region (49-100aa) weakens the interaction with Otu. These findings support the AlphaFold predictions.

Finally, to test whether the interaction between Sakura and Otu can be achieved solely through their N-terminal regions, we performed co-immunoprecipitation assay with Sakura(N) and Otu(N2). We discovered that Sakura(N) and Otu(N2) physically interact (**Fig 9F**). A reciprocal co-immunoprecipitation assay also confirmed their interaction (**Fig S13**), revealing that the interaction between Sakura and Otu can be established with just the 1-49aa of Sakura and the 1-339aa of Otu. Therefore, we conclude that Sakura interacts with Otu *in vivo,* and the N-terminal regions of both proteins are sufficient for their interaction.

Loss of *otu* phenocopies loss of *sakura*

Having established the interaction between Sakura and Otu, we were interested in whether they function together during oogenesis. We speculated that for them to interact and function together, Sakura and Otu must exhibit similar expression and localization patterns in ovaries. We generated two transgenic flies carrying full-length *otu-EGFP* or *otu(ΔTudor)-EGFP* transgenes; both constructs are C-terminally fused with EGFP and under the control of the *otu* promoter. We found that both Otu-EGFP and Otu(ΔTudor)-EGFP display similar expression and localization patterns to Sakura-EGFP (**Fig 1E**, 1F and **Fig 10A**). Like Sakura-EGFP, Otu-EGFP and Otu(ΔTudor)-EGFP are specifically expressed in germ cells, but not in follicle cells, and are localized to the cytoplasm, being enriched in the developing oocytes (**Fig 10A**). We did not observe any difference in localization patterns between Otu-EGFP and Otu(ΔTudor)-EGFP; suggesting that the Tudor domain is not crucial for Otu protein localization. Notably, the localization pattern exhibited by the transgenic Otu-EGFP generated in this study is consistent with a previous report (Glenn and Searles 2001).

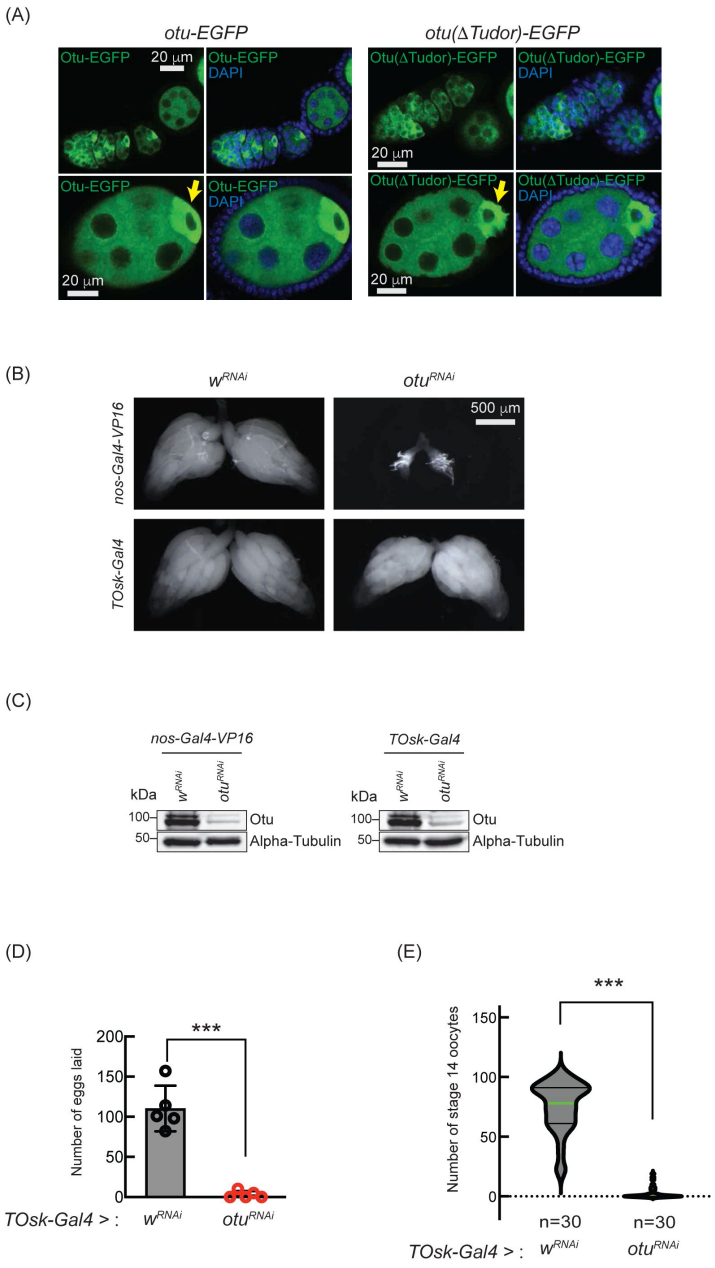

Fig 10.

Loss of *otu* phenocopies loss of *sakura*

(A) Confocal images of ovaries from *otu-EGFP* and *otu(ΔTudor)-EGFP* transgenic flies. Otu-EGFP and Otu(ΔTudor)-EGFP (green), DAPI (blue). Yellow arrows show the enrichment of Otu-EGFP and Otu(ΔTudor)-EGFP in developing oocytes. Scale bars: 20 μm. (B) Stereomicroscope images of dissected whole ovaries from w^{RNAi} (control) and otu^{RNAi} flies where RNAi knockdown was driven in the female germline with *nos-Gal4-VP16* or *TOsk-Gal4*. Scale bar: 500 μm. (C) Western blot of dissected ovary lysates. (D) Number of eggs laid by *TOsk-Gal4* > w^{RNAi} and *TOsk-Gal4* > otu^{RNAi} flies. Mean ± SD (n = 5). P-value < 0.001 (Student's t-test, unpaired, two-tailed) are indicated by ***. (E) Violin plots of the number of stage 14 oocytes produced in *TOsk-Gal4* > w^{RNAi} and *TOsk-Gal4* > otu^{RNAi} flies. n = 30. P-value < 0.001 (Student's t-test, unpa©red, two-tailed) is indicated by ***.

Previous studies have shown that mutations in *otu* lead to defects in germ cell division and differentiation, resulting in phenotypes including tumorous ovarioles (King and Riley 1982; King et al. 1986; Storto and King 1988; Steinhauer and Kalfayan 1992b). To study the role of *otu* specifically in the germline, we performed RNAi knockdown of *otu* in the germline driven by *nos-Gal4-VP16* (**Fig 10B** and **10C**). Interestingly, we found that germline depletion of *otu* results in rudimentary ovaries, similar to the loss of *sakura* (**Fig 2C**, **Fig 5A**, and **Fig 10B**). Furthermore, similar to *sakura* RNAi (**Fig 5**), *TOsk-Gal4*-driven *otu* RNAi knockdown did not affect ovary morphology (**Fig 10B**), but it resulted in a reduced number of eggs laid and stage 14 oocytes compared with control RNAi (w^{RNAi}) (**Figure 10D** and **10E**).

Given that *sakura* loss of function causes tumorous and germless ovarioles, apoptosis, piRNA pathway defects, *bam* misexpression, and reduced pMad levels (**Fig 3**, 4 and 7B-E), we asked whether similar defects occur upon *otu* depletion. Germline *otu* RNAi knockdown in 2-5 days old flies using *UAS-Dcr2* and *NGT-Gal4* lead to both germless (~70%) and tumorous (~30%) ovarioles, closely resembling the phenotype of *sakura* RNAi (**Fig S9A**). Similar germless and tumorous phenotypes were also observed in *nos-Gal4-VP16* > otu^{RNAi} flies (**Fig 11A**). In these otu^{RNAi} ovarioles, Bam-GFP expression was no longer restricted to 8-cell cysts, instead persisting throughout the germarium and egg chambers (**Fig 11A**). Additionally, $otu^{14/14}$ mutant GSCs showed reduced pMad levels (**Fig 11B**), and cleaved Caspase-3 staining revealed elevated apoptosis in *otu* RNAi ovaries (**Fig 11C**). Germline depletion of *otu* resulted in elevated expression of GFP and β-Gal produced by the *Burdock* sensor, indicating loss of piRNA-mediated transposon silencing (**Fig 11D**).

Together, these data demonstrate that *otu* loss-of-function closely phenocopies *sakura* loss-of-function, including defects in germline maintenance and differentiation, *bam* misexpression, reduced pMad signaling, and compromised piRNA pathway activity. These findings, along with physical interaction between Sakura and Otu (**Figs 8**, **9**, **S12**, and **S13**), suggest that they function together in regulating germline maintenance and differentiation.

To further explore their genetic interaction, we compared the ovariole phenotypes caused by single and double knockdowns of *sakura* and *otu* in the germline driven by *UAS-Dcr2* and *NGT-Gal4*. Individual knockdown of either gene resulted in ~70% germless and ~30% tumorous ovarioles in 2-5 days old flies (**Fig S9A**). Simultaneous knockdown of both genes increased the propotion of germless ovarioles to 86%, with a corresponding decrease in tumorous phenotypes to 14%, suggesting a synergistic enhancement of the germless phenotype. The number of GSC-like cells were not affected by the double knockdown of *sakura* and *otu* compared with their respective single knockdown (**Fig S9B**).

Sakura and Otu proteins do not depend on each other for their abundance

We investigated whether Sakura and Otu proteins depend on each other for their abundance. We performed Western blot analysis on ovaries with germline-specific knockdown of *sakura* or *otu*, driven by *TOsk-Gal4*. Otu protein levels were not reduced in $sakura^{RNAi}$ ovaries compared to control y^{RNAi} (**Fig S14A**), and conversely, Sakura levels were not decreased in otu^{RNAi} ovaries compared with control w^{RNAi} ovaries (**Fig S14B**). These results indicate that Sakura and Otu do not require each other for their protein expression or stability.

To further test this conclusion and to examine whether Otu enrichment to the posterior of egg chambers is affected by loss of *sakura*, we generated marked $sakura^{null}$ germline clones using the FLP-FRT system. Clones were marked by the absence of RFP, and experiments were performed in the flies expressing the *otu-EGFP* or *otu(ΔTudor)-EGFP* transgene in an otherwise wild-type ($otu^{+/+}$) background. Otu-EGFP fluorescence signal was comparable between $sakura^{null}$clones (*FRT82B*,

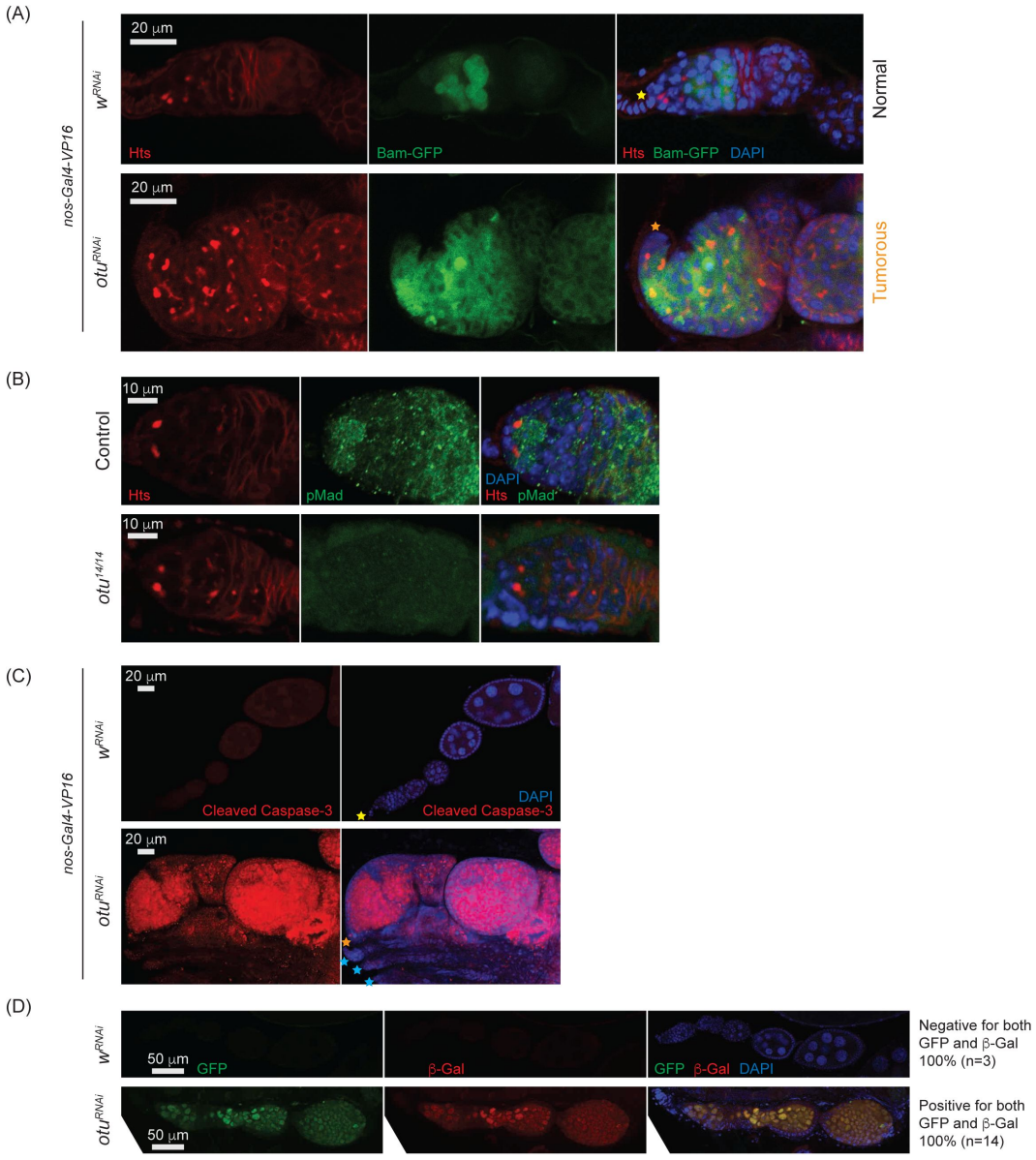

Fig 11.

Loss of *otu* results in low levels of pMad and derepression of *bam* in the germaria

(A) Confocal images of the ovaries from control (w^{RNAi}) and otu^{RNAi} flies harboring the *bam-GFP* reporter, where RNAi knockdown was driven in the female germline with *nos-Gal4-VP16*. Bam-GFP (green), Hts (red), and DAPI (blue). Scale bars: 20 μm. (B) Confocal images of germaria from control ($otu^{14/+}$) and $otu^{14/14}$mutant flies stained with anti-pMad (green) and anti-Hts (red) antibodies. Scale bars: 10 μm. (C) Confocal images of the ovaries from *nos-Gal4-VP16* > w^{RNAi} and *nos-Gal4-VP16* > otu^{RNAi} flies stained with anti-cleaved Caspase 3 antibody. Cleaved Caspase-3 (red) and DAPI (blue). Scale bars: 20 μm. (D) Confocal images of the ovaries from w^{RNAi} and otu^{RNAi} flies carrying the Burdock sensor, with RNAi driven in the female germline using *UAS-Dcr2*, *NGT-Gal4* and *nos-Gal4-VP16*. GFP (green), β-gal (red), and DAPI (blue). Scale bars: 50 μm. Three out of 3 tested control samples were negative for both GFP and β-gal, while 14 out of 14 tested otu^{RNAi} samples were positive for positive for GFP and β-gal.

sakura^{null}) and control clones (*FRT82B*) (**Fig 12A**). Similarly, Otu(ΔTudor)-EGFP levels were unaffected in *sakura*^{null} clones compared to the control clones (**Fig 12B**), confirming that Sakura is not required for Otu protein expression or stability.

Both Otu-EGFP and Otu(ΔTudor)-EGFP exhibited clear enrichment at the posterior of egg chambers in the control clones (*FRT82B*) —consistent with localization to the developing oocyte (**Fig 12A** and **12B**). This posterior enrichment was absent in *sakura*^{null}clones, demonstrating that Sakura is crucial for this process.

Sakura does not affect Otu's deubiquitinase activity in vitro

A previous study has shown that Otu possesses deubiquitinase activity (Ji et al. 2017). We asked whether Sakura regulates the Otu's deubiquitinase activity. To test this, we performed an in vitro deubiquitination assay using Ub-Rhodamine 110 as a model substrate. Consistent with the previous study (Ji et al. 2017), we detected a deubiquitinase activity in Otu that was ectopically expressed and purified from S2 cells (**Fig S15**). The presence of Sakura, purified from *E.coli,* did not affect Otu's deubiquitinase activity under these assay conditions. Additionally, Sakura itself did not exhibit deubiquitinase activity.

Discussion

In this study, we identified Sakura, encoded by a previously uncharacterized gene *CG14545*, as an essential factor for oogenesis and female fertility. We demonstrated that Sakura is specifically expressed in germline cells in the ovary, including GSCs, is localized to the cytoplasm, and is enriched in the developing oocytes. *sakura* homozygous null mutant flies are viable but completely female-sterile and male-fertile. Loss of *sakura*, either through null mutation or germline RNAi including in GSCs, results in rudimentary ovaries exhibiting germless and tumorous phenotypes.

The tumorous phenotype associated with the loss of *sakura* is characterized by an excess of GSC-like cells, which feature round spectrosomes, as well as cyst cells with branched fusomes (**Fig 3C**). The increased number of GSC-like cells in loss of *sakura* suggests dysregulation of GSC self-renewal and differentiation. Meanwhile, the presence of excess cyst cells with branched fusomes indicates abnormal differentiation and division of cysts. Differentiation of cystoblasts typically involves four mitotic divisions with incomplete cytokinesis, leading to 16 cyst cells interconnected by branched fusomes. The degree of fusome branching serves as a marker for the stages of cyst cell division, with increased branching from 2-cell to 16-cell cysts (de Cuevas and Spradling 1998). Notably, fusomes begin to degenerate and disappear after 16-cell cysts as the germline cyst enters the meiotic zone or region 2 of the germarium. The persistence of cyst cells with branched fusomes in *sakura*$^{null/null}$suggests that *sakura* is crucial for the proper division and differentiation of cysts, and we speculate that it is required for germline cysts to enter meiotic division.

Mosaic analysis of *sakura*^{null} indicates that *sakura* is intrinsically required for the establishment of GSCs in the ovary. When mutant clones were induced in PGC stage, significantly fewer *sakura*^{null} marked GSCs were observed in adult ovaries, suggesting that many *sakura*^{null} PGCs fail to survive or differentiate into GSCs. Furthermore, induction of *sakura*^{null} clones in adult ovaries led to a more rapid decline in marked *sakura*^{null} GSCs compared to controls, indicating that *sakura* is also intrinsically required for GSC maintenance (**Fig 6A**). Over time, germaria containing *sakura*^{null} GSC clones became increasingly tumorous, with an expanding population of *sakura*^{null} GSC-like cells (**Fig 6B** and **6C**). In contrast, the number of GSC-like cells across entire and all ovarioles regardless of whether GSCs in the niche remain, declined over time in *sakura*^{null} ovaries (**Fig S4B**). These results suggest that *sakura*^{null} GSCs initially undergo aberrant proliferation, leading

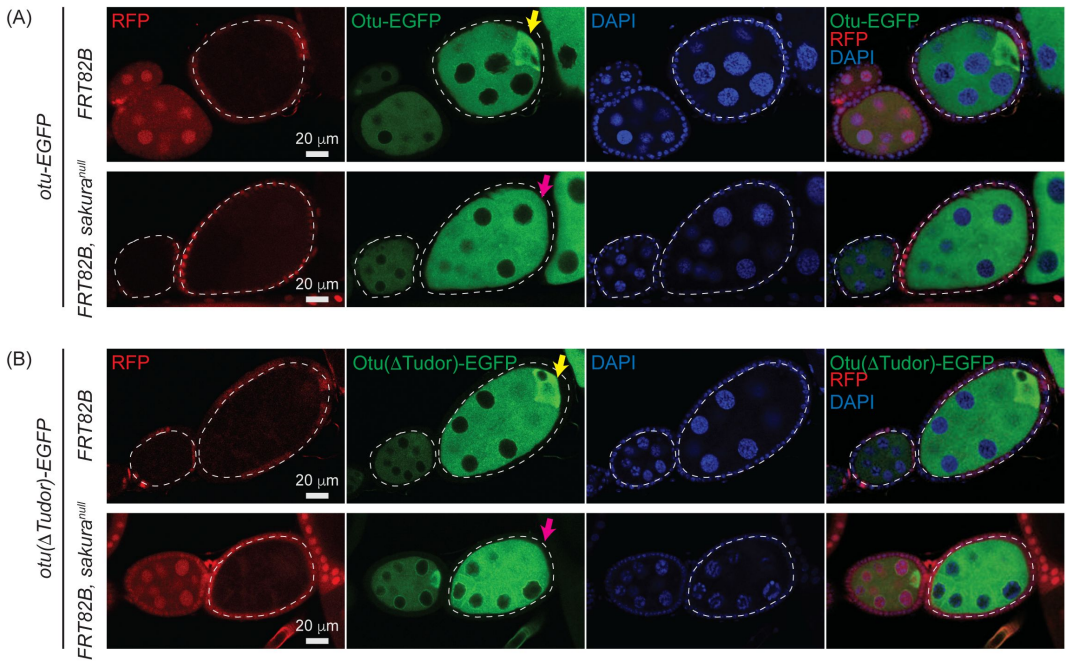

Fig 12.

Otu enrichment to the posterior within egg chambers is lost in *sakura*^{null}

Confocal images of egg chambers with germline clones of *sakura*^{null} expressing (A) Otu-EGFP or (A) (B) Otu(ΔTudor)-EGFP. Fly genotypes used: *hs-flp*/*w*; *otu-EGFP*/+; *FRT82B*, *ubi-RFP*/*FRT82B*. *hs-flp*/*w*; *otu-EGFP*/+; *FRT82B*, *ubi-RFP*/*FRT82B*, *sakura*^{null}. *hs-flp*/*w*; *otu(ΔTudor)-EGFP*/+; *FRT82B*, *ubi-RFP*/*FRT82B*. *hs-flp*/*w*; *otu(ΔTudor)-EGFP*/+; *FRT82B*, *ubi-RFP*/*FRT82B*, *sakura*^{null}. RFP (red), Otu-EGFP or Otu(ΔTudor)-EGFP (green), and DAPI (blue). Scale bars: 20 μm. Marked clones (RFP-negative) are outlined with white dotted lines. Yellow arrows indicate normal posterior enrichment of Otu-EGFP and Otu(ΔTudor)-EGFP signal; magenta arrows indicate the loss of this posterior enrichment in *sakura*^{null}clones.

to tumor formation, but are ultimately *sakura*^{null}GSCs and GSC-like cells are lost through a cell death mechanism, as evidenced by the elevated levels of cleaved Caspase-3 in *sakura*^{null} ovaries (**Fig 3F**).

Dpp/BMP signaling governs GSC self-renewal and cystoblast differentiation by repressing *bam* in GSCs and de-repressing it in daughter cystoblasts (**Fig 7A**). This process is mediated by the transcription factor Mad, which, when phosphorylated (pMad), translocates into the nucleus to repress *bam* transcription (Kirilly and Xie 2007; Kahney et al. 2019; Hinnant et al. 2020). Our findings indicate that Bam expression is not limited to 8-cell cysts but continues throughout the germarium in ovaries lacking *sakura* function (**Fig 7B** and **7C**). The misexpression of Bam in GSCs likely results from reduced levels of pMad in the GSCs (**Fig 7D**, and 7E). Given the low pMad levels observed upon loss of *sakura*, we propose that *bam* misregulation in GSCs occurs primarily at the transcriptional level, although Bam is also known to be subject to post-transcriptional regulation (Pek et al. 2009). The continued expression of Bam throughout the germarium, well beyond the GSC niche, suggests a failure to terminate *bam* expression at the 16-cell cyst stage —a developmental transition when *bam* is normally turned off. Thus, *sakura* mutants likely exhibit two distinct molecular defects contributing *bam* overexpression: (1) impaired Dpp/BMP signaling within the GSC niche, and (2) a failure to downregulate *bam* at 16-cell stage. Given the limited space within the GSC niche, the latter defect may be the predominant contributor to the observed *bam* overexpression. The molecular mechanism that silences *bam* at the 16-cell cyst stage remains poorly understood, and how *sakura* loss perturbs this regulation is unclear. The *sakura* mutant may therefore serve as a valuable model to investigate the mechanism that normally suppresses *bam* expression at the 16-cell stage.

Transposons are mobile genetic elements that, if not silenced, can generate DNA damage and genomic instability (Levin and Moran 2011). piRNAs derived from transposons and other repeats can target and silence transposon RNAs to preserve genome integrity in germ cells (Siomi et al. 2011). Loss of piRNAs leads to transposon derepression, resulting in increased DNA damage, which subsequently triggers cell death (Kang et al. 2018; Moon et al. 2018). Genetic damage in germ cells can cause developmental defects and diseases that may be inherited by the next generation. Thus, elimination of defective germ cells is crucial for maintaining germline integrity of a species (Chu et al. 2014; Ota and Kobayashi 2020). We found that loss of *sakura* results in reduced piRNA levels and loss of piRNA-mediated transposon silencing in the germline (**Fig 4**). The observed apoptosis, indicated by elevated cleaved Caspase-3 levels in *sakura* mutant ovaries (**Fig 3F**), suggest that desilencing of transposon due to reduced piRNA levels likely results in increased DNA damage, triggering cell death. We speculate that the germless phenotype in *sakura* mutants may partly arise from an apoptotic germline elimination program activated to maintain germline integrity.

In addition to its expression in GSCs and cysts in the germarium, Sakura is also expressed in germline cells in later-stage egg chambers (**Fig 1E-F**) and is required at this stage for proper oogenesis. When Sakura is depleted from region 2b of the germarium onward —leaving GSCs and early cyst cells intact—females have significantly fewer stage 14 oocytes and lay significantly fewer eggs (**Fig 5**). The failure to produce stage 14 mature oocytes likely stems from cytoskeletal disorganization that disrupt oocyte development, as evidenced by mislocalization of Orb (**Fig 5E**, **S7**, and **S12**). Notably, piRNA pathway mutants also exhibit similar Orb mislocalization (Ohtani et al. 2013). Therefore, the reduced piRNA levels (**Fig 4**) may contribute to the oocyte development defects, including Orb mislocalization, in *sakura* mutants. (**Fig 5E**).

Sakura does not possess any known protein domains. To infer its function, we identified Otu, a protein known to be crucial for oogenesis, as a protein partner of Sakura. Mutations in *otu* gene lead to a range of ovarian phenotypes, including germ cell loss, tumorous egg chambers filled with undifferentiated germ cells, defects in germlne sexual identity determination, abnormalities in nurse cell chromosome structure, and defects in oocyte determination (King and Riley 1982;

Storto and King 1988; Pauli et al. 1993; Glenn and Searles 2001). We showed that germline depletion of Otu via RNAi phenocopies loss of *sakura*. Similar to Sakura, loss of *otu* inhibits Dpp/BMP signaling, resulting in low pMad levels in GSCs and Bam de-repression (**Fig 11A-B**). Additionally, loss of *otu* also results in the loss of piRNA-mediated silencing, paralleling the effects of *sakura* loss. Furthermore, germline knockdown of *otu* yielded a similar ratio of germless ovaries as seen in *sakura-RNAi,* and simultaneous knockdown of both *otu* and *sakura* exacerbated the germless ovary phenotype (**Fig S9**). These observations raise the possibility that Sakura and Otu function together to regulate germ cell maintenance in the ovaries and are involved in Dpp/BMP signaling to balance stem cell renewal and differentiation.

Otu possesses deubiquitinase activity, catalyzed by its N-terminal Otu domain (Ji et al. 2017; Ji et al. 2019). In germ cells, Otu interacts with Bam, forming a deubiquitinase complex that deubiquitinates and thereby stabilizes CycA, promoting GSC differentiation. The predicted structure of Sakura and Otu complex suggests that the Mid domain of Sakura directly contacts the Otu domain of Otu (**Fig 9A**). We found that Sakura lacks a deubiquitinase activity and it does not directly affect Otu's deubiquitinase rate in our in vitro assays using Ub-Rhodamine 110 as a substrate (**Fig S15**). This does not preclude the possibility that Sakura may still influence Otu's deubiquitinase activity, potentially guiding Otu to its substrate and determining substrate specificity. Our in vitro assays may not have detected such specificity changes.

Otu is an RNA-binding protein whose deubiquitinase activity is enhanced by RNA binding (Ji et al. 2019). Bam, along with other proteins such as Bgcn, Mei-P26, and Sxl, binds —a key stem cell maintenance factor (Wang and Lin 2004)— and represses its translation in GSCs (Wang and Lin 2004; Li et al. 2009; Chau et al. 2012; Li et al. 2013). Bam and Otu form a protein complex (Ji et al. 2017). Future studies should explore whether Sakura modulates Otu's RNA-binding properties and its interaction with other proteins. Although Sakura is exclusively expressed in ovaries, particularly in germline cells including GSCs (**Fig 1**), Otu is broadly expressed in various tissues, including testes and gut (Steinhauer and Kalfayan 1992b). This restricted expression pattern suggests that Sakura may serve as a female germline-specific cofactor that enhances or modifies Otu's molecular functions. Identifying Otu's RNA targets and deubiquitinase substrates beyond CycA, as well as determining how Sakura binding influences these activities, will be key to elucidating their roles in oogenesis. One intriguing possibility is that Sakura regulates Otu's activity toward piRNA pathway components, thereby contributing proper piRNA biogenesis and function. Additionally, the Sakura-Otu complex may directly regulate essential post-transcriptional processes such as *sxl* alternative splicing and translational control of other oogenic RNAs.

In summary, this study identifies and characterizes the previously unknown gene *sakura*, which is specifically expressed in female germ cells and is essential for oogenesis and female fertility. Together with its protein partner Otu, Sakura likely regulates germline cell fate, maintenance, and differentiation.

Materials and Methods

Fly strains

We generated the *sakura*^{null} strain by introducing indels within the Sakura coding region using the CRISPR/Cas9 genome editing system, as we previously reported (Zhu et al. 2018a; Zhu et al. 2018b; Zhu et al. 2019b; Zhu and Fukunaga 2021). The transgenic *sakura-EGFP, otu-EGFP,* and *otu(ΔTudor)-EGFP* strains were created following previously published methods (Fukunaga et al. 2012; Kandasamy and Fukunaga 2016; Zhu and Fukunaga 2021). A fragment containing Sakura cDNA flanked by ~1 kbp upstream and ~1 kbp downstream genomic sequences was cloned. Fragments containing Otu and Otu(ΔTudor) cDNAs, flanked by ~2.5 kbp upstream and ~1

kbp downstream genomic sequences, were also cloned. The EGFP gene was fused in-frame to the C-terminus of the Sakura and Otu coding sequences within these fragments, which were then inserted into a pattB plasmid vector. The *sakura-EGFP* plasmid was integrated into the 51C1 site within the fly genome using the BDSC:24482 fly strain and the PhiC31 system, while the *otu-EGFP* and *otu(ΔTudor)-EGFP* plasmids were integrated into the 25C6 site of the genome using the attP40 fly strain and the PhiC31 system.

The *sakura RNAi* #1 (VDRC: v39727) and #2 (VDRC: v103660), *y-RNAi* (v106068), *TOsk-Gal4* (v 314033), Burdock sensor [*UAS-Dcr2; NGT-Gal4; nosGal4-VP16, nos>NLS_GF'_lacZ_vas-3'UTR_burdock-target*] (v 313217) strains were from Vienna *Drosophila* Resource Center. *w-RNAi* (BDSC: 35573), *otu-RNAi* (BDSC: 34065), *bam-RNAi* (BDSC: 33631), *cycA-RNAi* (BDSC: 29313), *UAS-Dcr-2; NGT-Gal4* (BDSC: 25751), *FRT82B/TM6C, Sb* (BDSC: 86313), otu^{14} (BDSC: 6025), *UASp-Mad-GFP* (BDSC: 604592), and *UASp-tkv.Q253D* (BDSC: 604934) were obtained from the Bloomington Stock Center. The *bam-GFP* reporter (DGRC: 118177) and *vasa-EGFP* knocked-in fly (DGRC: 118616) were from Kyoto *Drosophila* Stock Center. *sakura RNAi #2* was much healthier than *sakura RNAi #1* without being driven with any Gal4 for some reasons and thus we chose to use the RNAi #2 line in most of this study.

sakura-EGFP does not cause any phenotypes in the background of $sakura^{+/+}$ and $sakura^{null/+}$.

Fertility assay

The female fertility assay was performed as previously described (Zhu et al. 2018b; Liao et al. 2019; Zhu et al. 2019a; Zhu and Fukunaga 2021). Briefly, five test virgin females of each test genotype were mated with three wild-type (OregonR) males in a cage with a 6-cm grape juice agar plate supplemented with wet yeast paste. The agar plates were replaced daily, and the number of eggs laid on the third plate (on day 3) was recorded. After incubation at 25°C for an additional day, the number of hatched eggs was counted. At least three cages per genotype were tested.

For the male fertility assay, a single test male was mated with five wild-type (OregonR) virgin females in each vial, following previously published methods (Zhu et al. 2018b; Zhu et al. 2019a; Zhu and Fukunaga 2021). After 3 days, the females were transferred to a new vial (vial 1). Every two days, they were transferred to a new vial until a total of four vials were obtained. After 2 days in the fourth vial, the females were removed, and the total number of progenies emerging from these four vials was counted. At least five males per genotype were tested.

Sakura and Otu antibodies

We expressed a recombinant full-length Sakura protein as an N-terminal 6xHis-tagged protein in *E. coli* using a modified pET vector and purified it using Ni-sepharose (GE Healthcare) and HiTrapQ HP (GE Healthcare) columns (Fukunaga and Doudna 2009). Recombinant Otu fragments (145-405aa and 406-853aa) were similarly expressed as N-terminally 6xHis-MBP-fusion proteins in *E. coli* and purified using Ni-sepharose. These purified proteins were used as antigens to generate polyclonal anti-Sakura and anti-Otu sera in rabbits (Pocono Rabbit Farm & Laboratory, Inc.). The rabbit polyclonal anti-Sakura antibodies were affinity purified using His-MBP-Sakura recombinant protein and Affigel-15 (Bio-rad), following the manufacturer's instructions. Rabbit anti-Otu sera were first pre-cleared with purified His-MBP protein bound to Affigel-15, and the unbound fraction was affinity purified using purified His-MBP-Otu fragments (145-405aa and 406-853aa) and Affigel-15.

Immunostaining

Stereomicroscope images of dissected ovaries were taken using Leica M125 stereomicrocsope. Ovaries from 2- to 5-day-old, yeast-fed females were hand-dissected in 1X PBS (137 mM NaCl, 2.7 mM KCl, 10 mM Na_2HPO_4, 1.8 mM KH_2PO_4, pH 7.4) at room temperature. The dissected ovaries

were fixed in a fixative buffer (4% formaldehyde, 15 mM PIPES (pH 7.0), 80 mM KCl, 20 mM $NaCl_2$, 2 mM EDTA, and 0.5 mM EGTA), incubated for 30 minutes at room temperature with gentle rocking. After fixation, the ovaries were rinsed three times with PBX (0.1% Triton X-100 in 1X PBS) and then incubated in a blocking buffer (2% donkey serum in 3% BSA [w/v], 0.02% NAN_3 [w/v] in PBX) for 1 hour at room temperature. Then, the ovaries were incubated with primary antibodies diluted in the blocking buffer overnight at 4°C. The following day, the ovaries were rinsed three times with PBX and incubated with Alexa Fluor-conjugated secondary antibodies for 2 hours. The ovaries were rinsed three times with PBX and then mounted in VECTASHIELD® PLUS antifade mounting medium with DAPI (H-2000, Vector lab). Confocal images were acquired on a Zeiss LSM700 confocal microscope at the Johns Hopkins University School of Medicine Microscope Facility.

The primary antibodies used for immunostaining were mouse anti-HTS (1B1) (DSHB, AB_528070, dilution: 1/100), mouse anti-Bam (DSHB, AB_10570327, 1/20), mouse anti-CycA (DSHB, AB_528188, 1/100), rat anti-Vasa (DSHB, AB_760351, 1/100), rat anti-DE Cadherin (DCAD2) (DSHB, AB_528120, 1/20), rabbit anti-pMad (Cell Signaling, Phospho-SMAD1/5 (Ser463/465) mAb #9516, 1/200,), and rabbit anti-cleaved caspase-3 (Cell Signaling, Cleaved Caspase-3 (Asp175) #9661, 1/200). Secondary antibodies used were Alexa Fluor 488 Donkey anti-Mouse Igg (ThermoFisher, A21202, 1/100), Alexa Fluor 594 Donkey anti-Rat Igg (ThermoFisher, A21209, 1/100), Alexa Fluor 594 Donkey anti-Mouse Igg (ThermoFisher, A21203, 1/100), and Alexa Fluor 594 Donkey anti-Rabbit Igg ThermoFisher, A21207, 1/100). Rhodamine phalloidin (ThermoFisher, R415, 1/100) was used to stain F-Actin.

While our Sakura antibody detects Sakura in immunostaining, it seems to detect some other proteins as well. Since we have Sakura-EGFP fly strain, which rescues *sakura*^{null} phenotypes, we relied on Sakura-EGFP rather than anti-Sakura antibodies immunostaining to examine Sakura expression and localization.

Germline clonal analysis

We generated *sakura*^{null} mutant clones using FLP/FRT-mediated recombination (Rubin and Huynh 2015). To induce *sakura*^{null} GSC clones, 3-day-old female flies of the genotype *hs-flp*/*w*; +; *FRT82B, ubi-GFP/FRT82B, sakura*^{null} were heat-shocked at 37°C for 1 hour, twice daily, with an 8-hour interval between heat shocks. Female flies of the genotype *hs-flp*/*w*; +; *FRT82B, ubi-GFP/FRT82B* were used as controls. Ovaries were dissected and stained 4, 7, and 14 days after clone induction. To induce primordial germ cell (PGC) clones, early third-instar larvae were subjected to the same heat shock regime, then allowed to develop to adulthood. Ovaries were dissected and analyzed at 3 to 4 days after eclosion.

To induce *sakura*^{null} mutant clones in the presence of *otu-EGFP* or *otu(ΔTudor)-EGFP* transgenes, 3-day-old female flies with the genotype *hs-flp*/*w*; *otu-EGFP*/+; *FRT82B, ubi-RFP*/*FRT82B, sakura*^{null} and *hs-flp*/*w*; *otu(ΔTudor)-EGFP*/+; *FRT82B, ubi-RFP*/*FRT82B, sakura*^{null} were heat-shocked under the same conditions. Control genotypes were *hs-flp*/*w*; *otu-EGFP*/+; *FRT82B, ubi-RFP*/*FRT82B* and *hs-flp*/*w*; *otu(ΔTudor)-EGFP*/+; *FRT82B, ubi-RFP*/*FRT82B* were used as controls. Flies were dissected 3-4 days after clone induction.

Western blot

Lysates of hand-dissected ovaries and tissues were prepared by homogenizing in RIPA buffer (50 mM Tris-HCl [pH 7.4], 150 mM NaCl, 1% [v/v] IGEPAL CA-630, 0.1% [w/v] sodium dodecyl sulfate (SDS), 0.5% [w/v] sodium deoxycholate, 1 mM ethylenediaminetetraacetic acid (EDTA), 5 mM dithiothreitol, and 0.5 mM phenylmethylsulfonyl fluoride (PMSF)) (Kandasamy et al. 2017; Zhu et al. 2018b). The homogenates were centrifuged at 21,000g at 4°C for 10 min, and the protein concentration of the supernatant was determined using the BCA protein assay kit (Pierce) as needed. Fifteen µg of total protein was loaded per lane for Western blot. The sources and dilutions of the primary antibodies were as below. Rabbit anti-Sakura (1/10000, generated in this study),

rabbit anti-Otu (1/10000, generated in this study), rabbit anti-alpha-Tubulin [EP1332Y] (1/10000, Abcam, ab52866), mouse anti-alpha-Tubulin [12G10] (1/10000, DSHB, AB_1157911), mouse anti-FLAG (1/10000, Sigma, F1804), mouse anti-HA (1/10000, Sigma, H3663), and mouse anti-GFP [GF28R] (1/3000, Invitrogen, 14-6674-82). IRDye 800CW goat anti-mouse IgG, IRDye 800CW goat anti-rabbit IgG, IRDye 680RD goat anti-mouse, and IgG IRDye 680RD goat anti-rabbit were used as secondary antibodies. The membranes were scanned using the Li-Cor Odyssey CLx Imaging System.

Mass spectrometry

Immunoprecipitation of Sakura-EGFP protein was performed using the GFP-Trap Magnetic Agarose Kit (Proteintech, gtmak-20) on dissected ovaries from flies harboring *sakura-EGFP* transgene, with *w1118* flies as controls. Ovaries were homogenized in 200 µL ice-cold lysis buffer (10 mM Tris-HCl [pH 7.5], 150 mM NaCl, 0.5 mM EDTA, 0.05% [v/v] IGEPAL CA-630) containing 1× protease inhibitor cocktail (100× protease inhibitor cocktail contains 120 mg/ml 1 mM 4-(2-aminoethyl) benzene sulfonyl fluoride hydrochloride (AEBSF), 1 mg/ml aprotinin, 7 mg/ml bestatin, 1.8 mg/ml E-64, and 2.4 mg/ml leupeptin). After homogenization, the tubes were placed on ice for 30 minutes, and the homogenates were extensively pipetted every 10 minutes. The lysates were then centrifuged at 17,000x g for 10 minutes at 4°C. The supernatants were transferred to pre-chilled tubes, and 300 µL dilution buffer (10 mM Tris/Cl pH 7.5, 150 mM NaCl, 0.5 mM EDTA) supplemented with 1x protease inhibitor cocktail were added. The diluted lysates were then added to the GFP-trap magnetic beads in 1.5 mL tubes and rotated for 1 hour at 4°C. After separating the beads with a magnetic tube rack, the beads were washed three times with 500 µL wash buffer (10 mM Tris/Cl pH 7.5, 150 mM NaCl, 0.05 % [v/v] IGEPAL CA-630). Proteins were eluted with 40 µL acidic elution buffer (200 mM glycine pH 2.5) followed by immediate neutralization with 5 uL neutralization buffer (1 M Tris pH 10.4).

As a quality control before mass spectrometry, ~5 µL of the samples were mixed with an equal volume of 2× SDS-PAGE loading buffer (80 mM Tris-HCl [pH 6.8], 2% [w/v] SDS, 10% [v/v] glycerol, 0.0006% [w/v] bromophenol blue, 2% [v/v] 2-mercaptoethanol), heated at 95 °C for 3 min, and run on 4–20% Mini-PROTEAN® TGX™ Precast Protein Gels (Biorad, #4561094). Silver staining was then performed by using Pierce™ Silver Stain Kit (ThermoFisher, 24612) to assess the quality of the immunoprecipitated protein samples. Mass spectrometry was conducted at the Mass Spectrometry Core at the Department of Biological Chemistry, Johns Hopkins School of Medicine, as previously described (Zhu and Fukunaga 2021).

Co-immunoprecipitation

For co-immunoprecipitation of endogenous Sakura protein, wild-type ovaries (*w1118*) were homogenized in RIPA buffer, centrifuged at 21,000g at 4°C for 10 min, and the clear supernatant protein lysates were used for immunoprecipitation. Four µg of rabbit anti-Sakura and normal rabbit IgG (Cell Signaling, #2729) were incubated with 50 µL of Dynabeads Protein G (ThermoFisher, 10004D) for 20 min at room temperature. The beads were washed once with PBST (1x PBS with 0.1% Tween-20). The ovary lysate supernatant was then incubated with the washed beads at room temperature for 30 min, followed by three washes with PBST. The proteins were eluted with 2x SDS-PAGE loading buffer (80 mM Tris-HCl [pH 6.8], 2% [w/v] SDS, 10% [v/v] glycerol, 0.0006% [w/v] bromophenol blue, 2% [v/v] 2-mercaptoethanol) and heated at 70°C for 10 min. After bead separation using a magnetic tube rack, the eluted proteins in 2x SDS-PAGE loading buffer were heated again at 95°C for 3 min.

Transient protein expression in S2 cells was performed using the pAc5.1/V5-HisB plasmid vector (Invitrogen). A total of 1 µg plasmids were transfected using the Effectene transfection reagent (Qiagen, 301425). Three days after transfection, cells were harvested and lysed with ice-cold lysis buffer supplemented with 1× protease inhibitor cocktail. The cell lysates were then centrifuged at 17,000x g for 10 min at 4°C, and the clear supernatants were collected for immunoprecipitation.

For anti-HA immunoprecipitation, supernatants were incubated with 25 µL (0.25 mg) of Pierce™ Anti-HA Magnetic Beads (ThermoFisher, 88837) at room temperature for 30 min. The beads were then washed three times with TBST (1x TBS [0.05 M Tris/HCl and 0.15 M NaCl, pH 7.6] with 0.05% Tween-20). For anti-FLAG immunoprecipitation, 2 µg of mouse anti-FLAG (1/10000, Sigma, F1804) was incubated with 50 µL of Dynabeads Protein G (ThermoFisher, 10004D) for 10 min at room temperature. The beads were washed once with PBST. The S2 cell lysate supernatant was incubated with the washed beads at room temperature for 15 min. The beads were washed three times with PBST. In both anti-HA and anti-FLAG immunoprecipitations, proteins were eluted with 2× SDS-PAGE loading buffer. For anti-HA, the beads in 2x SDS-PAGE loading buffer were heated at 95°C for 7 min. For anti-FLAG, the beads were heated at 70°C for 10 min, then were separated using a magnetic tube rack. The eluted proteins in 2x SDS-PAGE loading buffer were heated again at 95°C for 3 min.

While the anti-Otu antibody worked in immunoprecipitation from ovaries, in subsequent in anti-Sakura Western blot after anti-Otu IP, Otu antibody light chain bands often overlapped with the Sakura band. Using epitope-tags in S2 cells avoided this issue.

Small RNA and mRNA sequencing

Poly-A+ mRNA purification was performed as previously described (Fukunaga et al. 2012). Small RNA libraries and poly-A+ mRNA libraries were prepared, sequenced on Hiseq2500 (Illumina), and analyzed, as previously reported (Fukunaga et al. 2014; Kandasamy et al. 2017; Liao et al. 2018; Zhu et al. 2018a; Zhu et al. 2018b; Liao et al. 2019; Zhu et al. 2019a; Zhu et al. 2019b). SRA accession number for these datasets is PRJNA1156618.

RT-PCR

Total RNAs from testes and ovaries were prepared using miRVana (Thermo Fisher Scientific). RNAs were treated with Turbo DNase (Thermo Fisher Scientific) to remove potential genomic DNA contamination. A total of 1 µg of RNA was reverse-transcribed into cDNA using SuperScript^{TM} VILO^{TM} MasterMix (Thermo Fisher Scientific). To assess *sxl* alternative splicing, PCR was performed using GoTaq Green Master Mix (Promega) with the primers *sxl*-F (CTCACCTTCGATCGAGGGTGTA) and *sxl*-R (GATGGCAGAGAATGGGAC).

In vitro deubiquitination assay

C-terminally 6xHis-tagged recombinant Sakura protein was expressed in *E. coli* using a modified pET vector and was purified using Ni-sepharose. N-terminally 3xHA-HRV3Csite-3xFLAG-tagged Otu protein and a negative control, N-terminally 3xHA-HRV3Csite-3xFLAG-tagged firefly luciferase protein, were expressed in S2 cells using pAc5.1/V5-HisB vector. The proteins were immunoprecipitated using Pierce™ Anti-HA Magnetic Beads (ThermoFisher, 88837) as described previously, with a more stringent washing step to effectively remove interacting proteins. The beads were washed six times with a high salt wash buffer (TBST with 800 mM NaCl). The proteins were eluted by cleaving off 3xHA tag with 25 nM GST-HRV3C protease in a cleavage buffer (25mM Tris-HCl pH 7.4, 150 mM NaCl, 5% glycerol, 2mM EDTA), incubated at 4°C with rotation for 6 hours. An equal volume of 100% glycerol was added to the eluted protein.

Purified proteins, including Otu, luciferase, and Sakura, were mixed with Ub-Rhodamine 110 (Ubiquitin-Proteasome Biotechnologies, M3020) in a total volume of 30 µL in reaction buffer (20 mM Tris-HCl, pH 7.5, 200 mM NaCl, 5 mM $MgCl_2$, 2 mM DTT). The mixture was added to a black 384-well low-volume plate. Fluorescence measurements were taken using SpectraMax i3x Multi-Mode Microplate Reader at 37°C, with excitation and emission wavelengths set at 485/20 and 530/20 nm respectively. The fluorescence intensity for each condition was averaged from triplicates and plotted as a function of time.

Fig S1.

sakura mRNA expression pattern.

Data obtained from *http://flybase.org/reports/FBgn0040602.htm*.

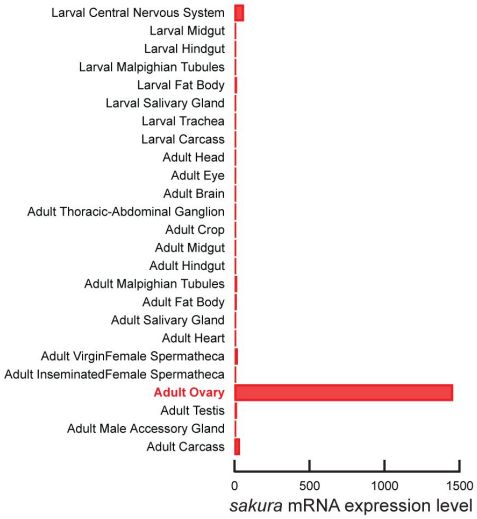

Fig S2.

Male fertility assay.

The numbers of the progeny flies obtained from crosses between test males and wild-type (OregonR) virgin females are shown. Mean ± SD (n = 5).

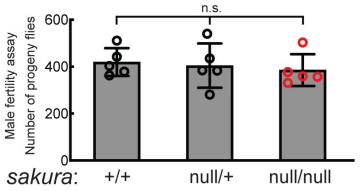

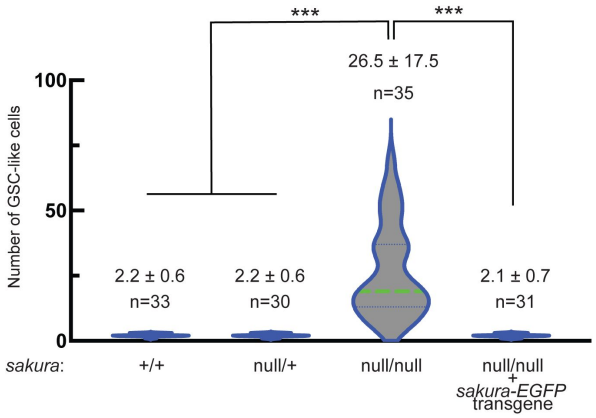

Fig S3.

sakura^{null} ovaries are tumorous

Violin plots of GSC-like cell numbers in germaria of indicated genotypes of 2-5 days old flies. Mean ± SD and the biological replicate number n are also shown. P-value < 0.001 (Student's t-test, unpaired, two-tailed) is indicated by ***.

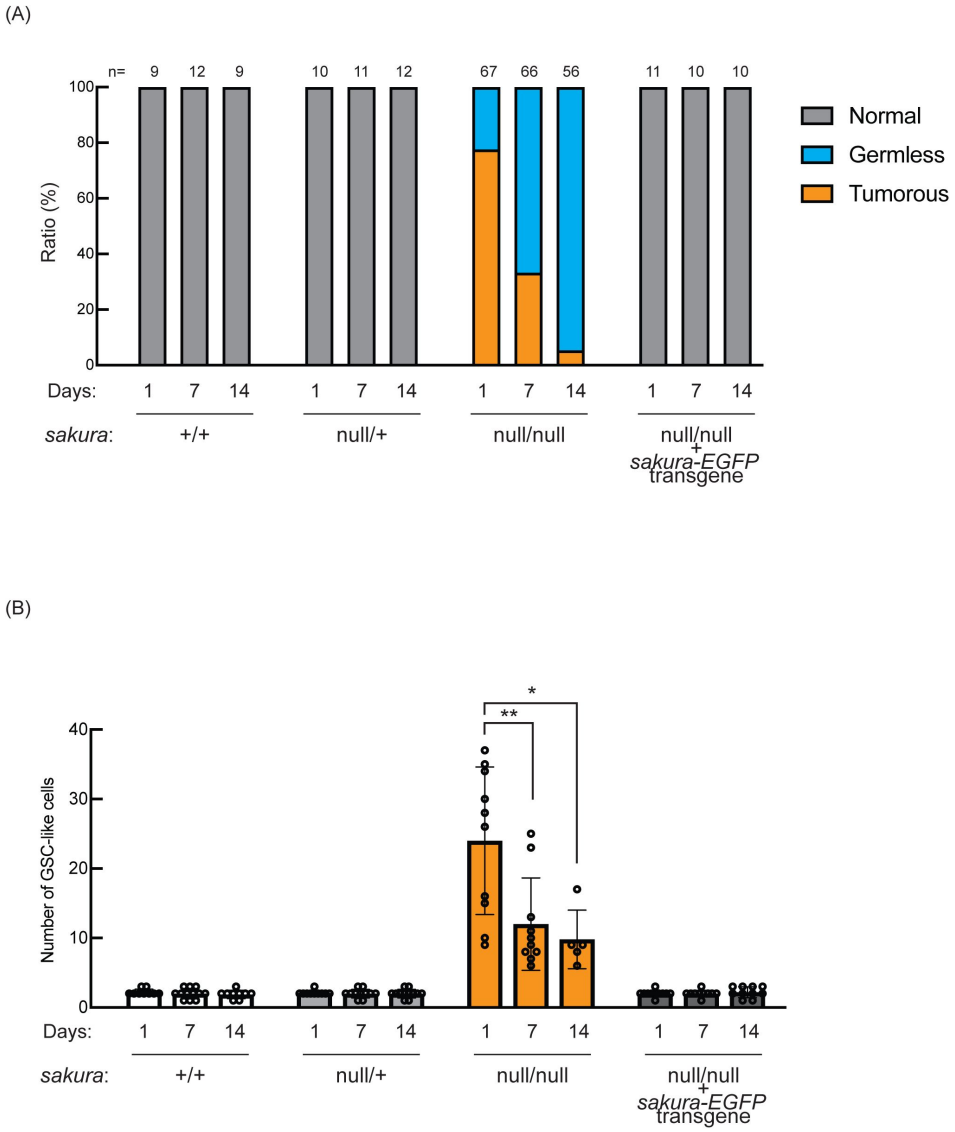

Fig S4.

The ratio of germless ovarioles increases over time in *sakura*^{null} ovaries

(A) Ratio (%) of normal, germless, and tumorous ovarioles of the indicated genotypes at 0-1 days, 7 days, and 14 days post-eclosion. (B) Quantification of GSC-like cell numbers in ovarioles of the indicated genotypes of at 0-1 days, 7 days, and 14 days post-eclosion. Germless ovarioles were excluded from this analysis.

Fig S5.

Sex-specific alternative splicing of *sxl* is dysregulated in *sakura*^{null} ovaries

Sex-specific alternative splicing of *sxl* was analyzed by RT-CPR followed by agarose gel electrophoresis and SYBR Safe staining. Ovaries from controls and *sakura-EGFP* rescue flies showed the expected female-specific *sxl* isoform, while testes from control flies exhibited the male-specific isoform. *sakura*^{null} ovaries showed increased expression of the male-specific isoform and reduced levels of female-specific isoform.

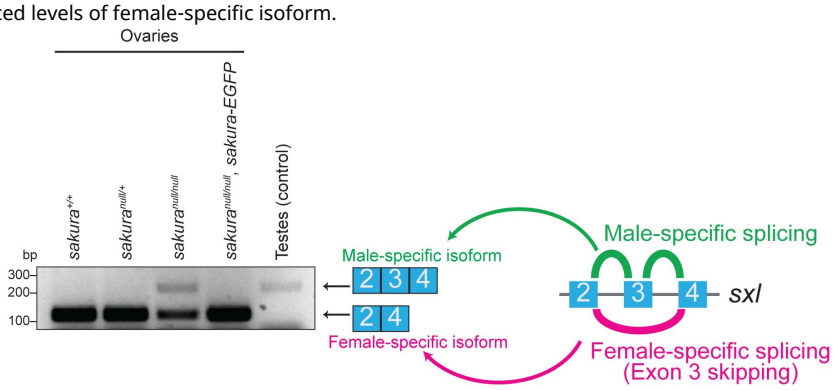

Fig S6.

sakura is important for oogenesis in later-stage egg chambers

Confocal images of ovaries from *sakura* RNAi knockdown flies (*UAS-Dcr2*, *TOsk-Gal4* > *sakura* ^{RNAi}) stained with phalloidin (F-Actin) and anti-Orb antibodies. F-Actin (red), Orb (green), and DAPI (blue). Yellow arrows indicate normal Orb enrichment at the posterior of developing oocytes. White arrowheads indicate egg chambers exhibiting cytoskeletal disorganization. Scale bars: 50 μm.

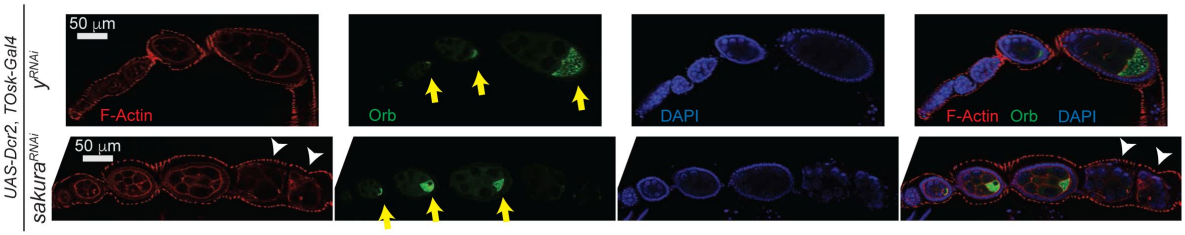

Fig S7.

sakura^{null} clone germline cells intrinsically cause tumorous phenotype

Number of GFP-positive GSC-like cells in germaria with marked (GFP-negative) GSCs of the indicated genotypes at 4, 7, and 14 days after clone induction. GSC-like cells containing round spectrosome were identified through immunostaining with anti-Hts antibody.

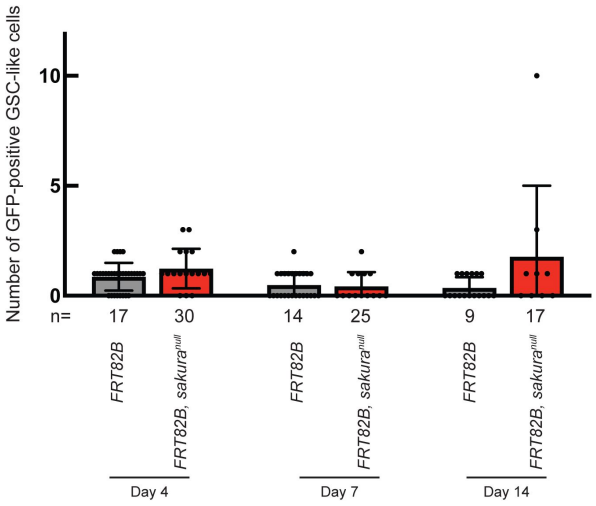

Fig S8.

Bam is not misexpressed in TOsk-Gal4 > *sakura*^{RNAi} egg chambers.

Confocal images of ovaries from *sakura* RNAi knockdown flies driven by *UAS-Dcr2* and *TOsk-Gal4*, stained with anti-Bam and anti-DE-Cadherin (DE-Cad) antibodies. *y-RNAi* was used as a control. Bam (green), DE-Cad (red), and DAPI (blue). Cyan arrowheads indicate high Bam expression in 8-cell cysts within the germarium. White arrowheads indicate egg chambers with cytoskeletal disorganization. Scale bars: 50 μm.

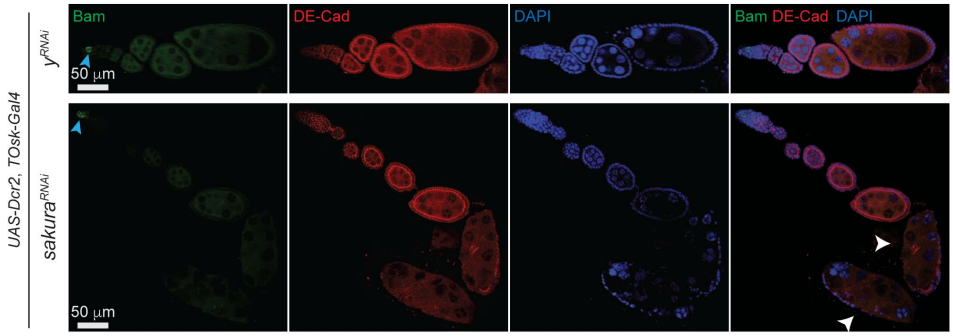

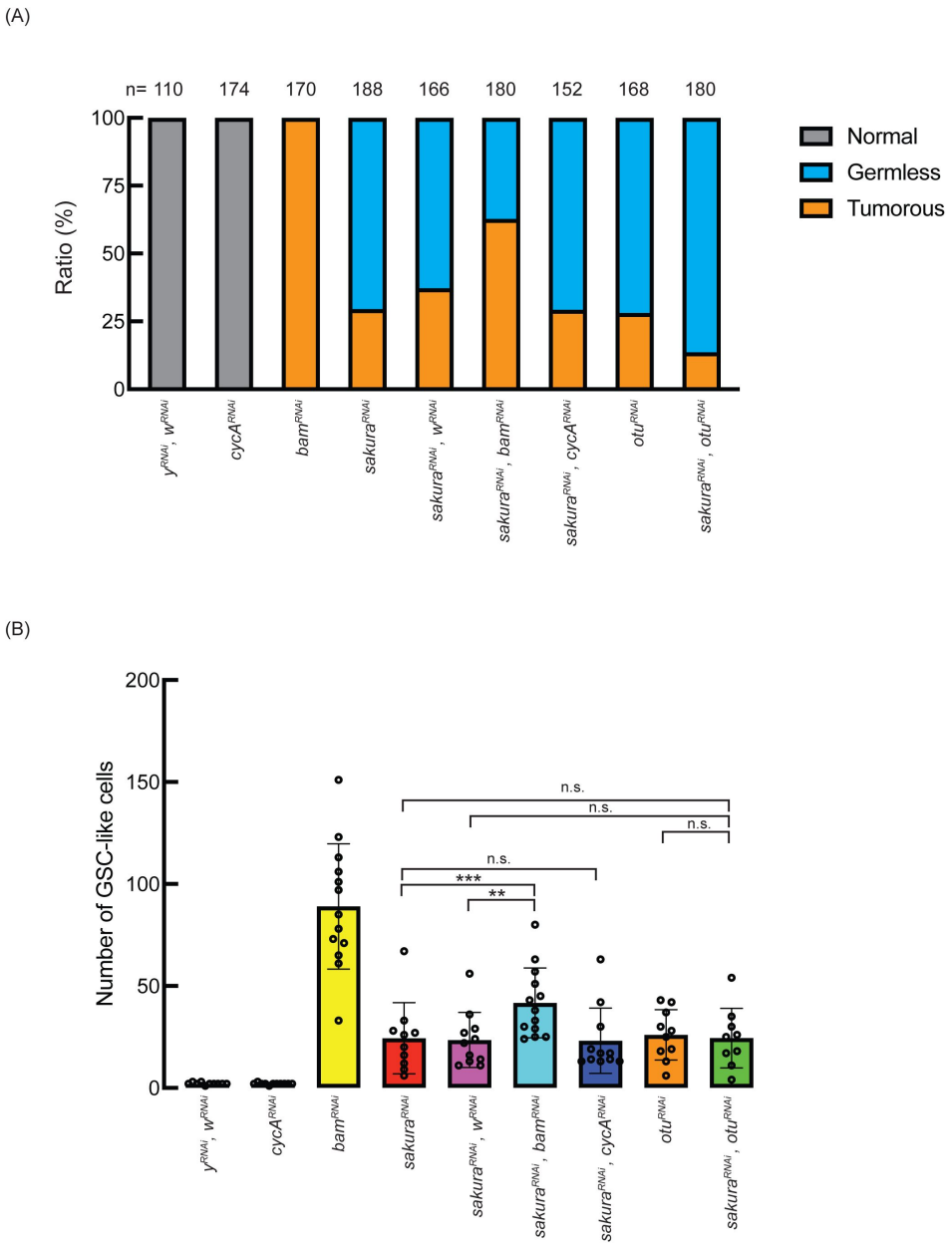

Fig S9.

Ratio of germless and tumorous phenotypes from double RNAi knockdown of *sakura* with *bam*, *cycA*, or *otu*

(A) Ratio (%) of normal, germless, and tumorous ovarioles in double RNAi knockdown of *sakura* with *bam, cycA,* or *otu. UAS-Dcr2* and *NGT-Gal4* was used to drive RNAi knockdown in the germline. n is the total number of ovarioles examined for the indicated genotypes of 2-5 day-old flies. (B) Quantification of GSC-like cell number in germaria of indicated genotypes of 2-5 day-old flies. Germless ovarioles were excluded from this analysis.

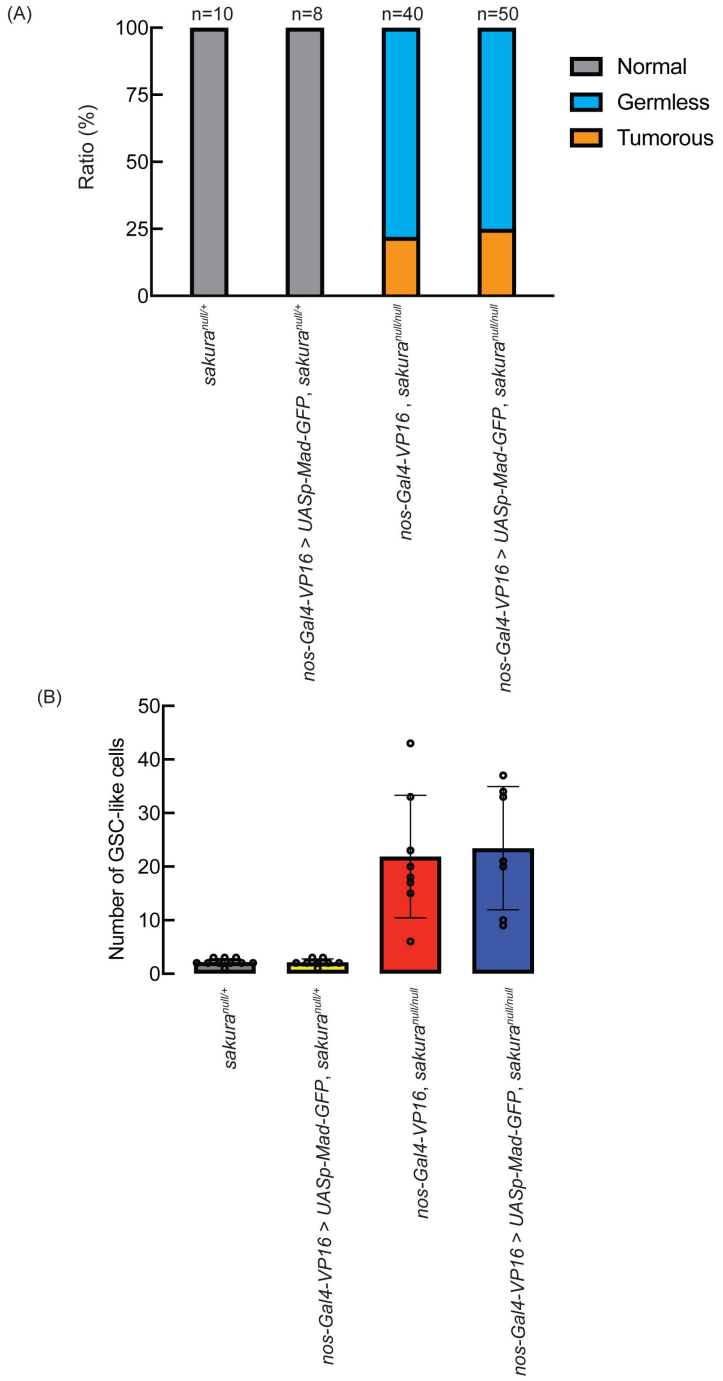

Fig S10.

nos-Gal4-VP16 > UASp-Mad-GFP did not rescue the *sakura*^{null} phenotypes

(A) Ratio (%) of normal, germless, and tumorous ovarioles in the indicated genotypes of 2-5 day-old flies. n denotes the total number of ovarioles examined for each genotype. (B) Quantification of GSC-like cell number in germaria of the indicated genotypes from 2-5 day-old flies. Germless ovarioles were excluded from this analysis.

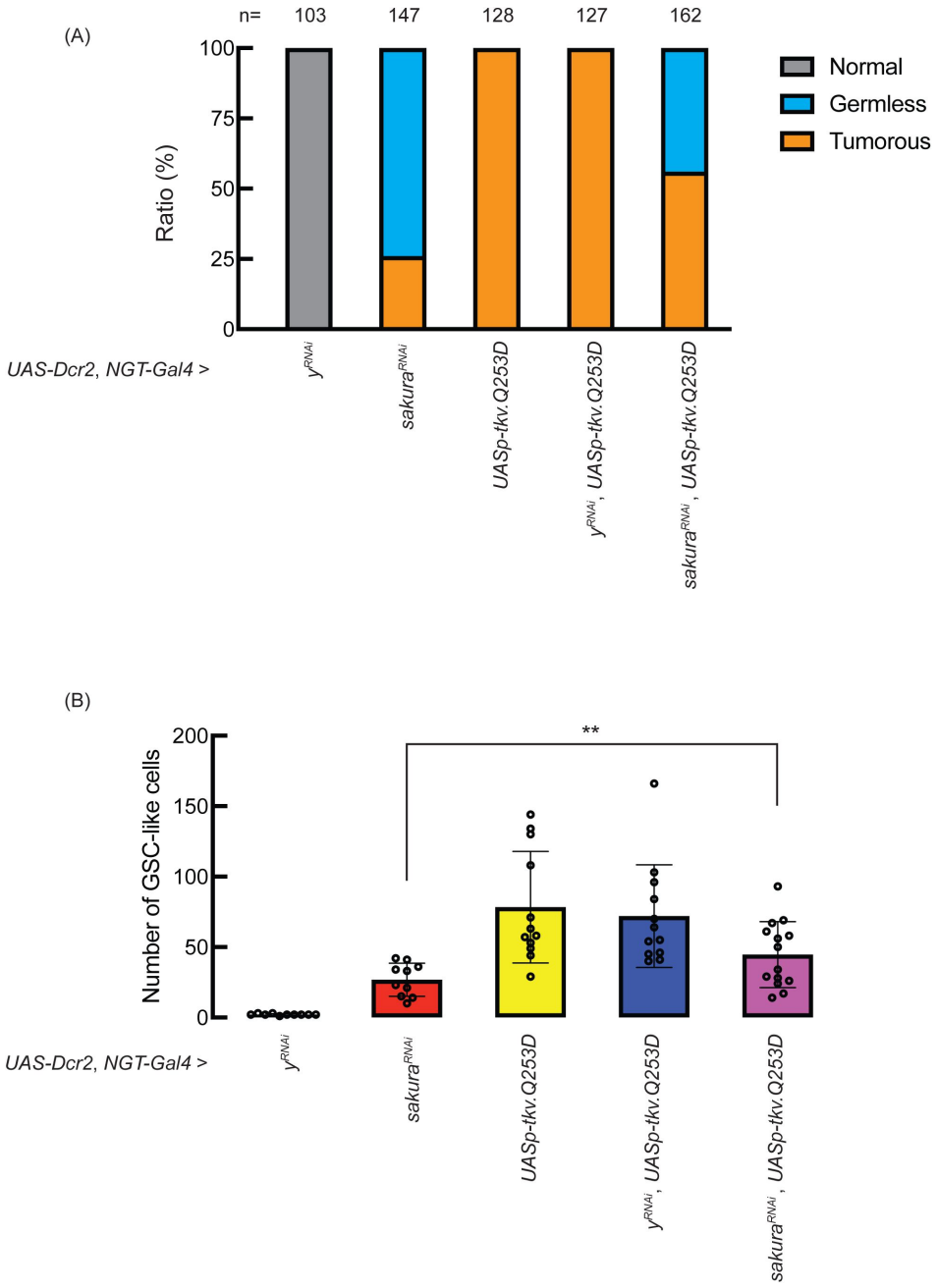

Fig S11.

Ratio of germless and tumorous phenotypes in *sakura* RNAi knockdown and *NGT-Gal4 > UASp-tkv.Q253D*.

(A) Ratio (%) of normal, germless, and tumorous ovarioles in the indicated genotypes of 2-5 day-old flies. RNAi knockdown and UASp-tkv.Q253D expression were driven with *UAS-Dcr2* and *NGT-Gal4*. n indicates the total number of ovarioles examined for each genotype. (B) Quantification of GSC-like cell number in germaria of the indicated genotypes from 2-5 day-old flies. Germless ovarioles were excluded from this analysis.

Fig S12.

anti-Otu Western blot of dissected ovary lysates.

(A) Western blot of dissected ovary lysates. (B) Western blot of dissected ovary lysates prepared from flies 2-5 hours and 3-7 days post eclosion and co-IP with anti-Sakura. The SDS-PAGE gel was run for a longer duration to better separate the 104 kDa and 98 kDa Otu isoforms. In 2-5 hour ovaries, the 104 kDa Otu isoform is more abundant, while in 3-7 day ovaries, the 98 kDa isoform predominates. Both Otu isoforms co-IPed with Sakura. The same 3-7 day ovary input and IP samples used for **Fig 9B** were used for anti-Otu and anti-Alpha-Tubulin Western. The anti-Sakura image is the same as shown in **Fig 9B**.

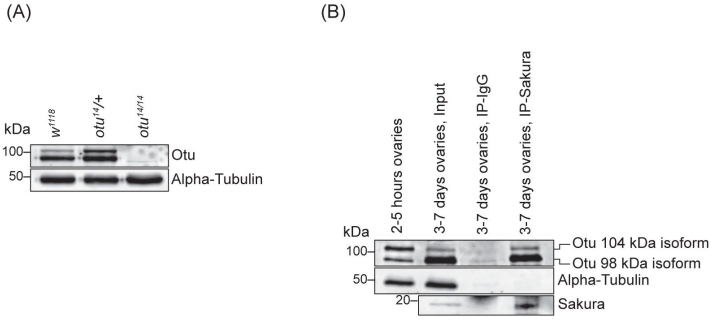

Fig S13.

Co-immunoprecipitations assay to test interaction between N-terminal fragments of Sakura and Otu in S2 cells

Co-immnuprocepitation assay using beads bound with anti-FLAG antibody followed by Western blotting. S2 cell lysates expressing mCherry-3xHA were used as controls. This is the reciprocal co-immunoprecipitation of **Fig 9F**.

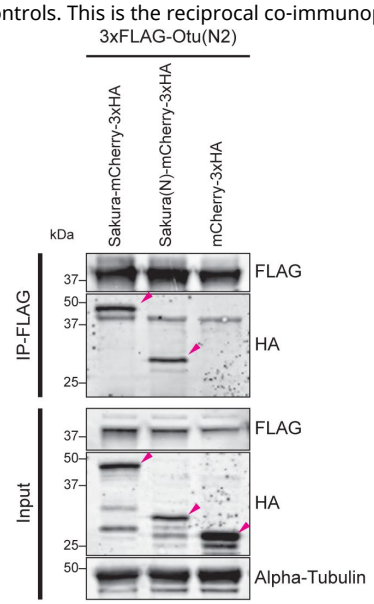

Fig S14.

Depletion of Sakura does not deplete Otu and depletion of Otu does not deplete Sakura

(A) Western blot of dissected ovary lysates. The same samples used for **Fig 5B** were used for anti-Otu Western. The anti-Sakura and anti-Alpha tubulin images are the same as shown in **Fig 5B**. (B) The same samples used for **Fig 10C** were used for anti-Sakura Western. The anti-Otu and anti-Alpha tubulin images are the same as shown in **Fig 10C**.

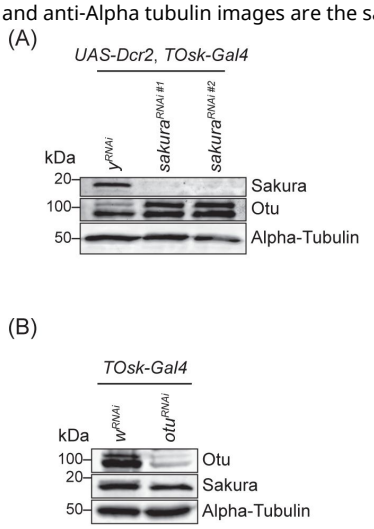

Fig S15.

In vitro deubiquitination assay.

The mean fluorescence intensity of three replicates was plotted. Error bars (+/-) are standard deviations. Firefly Luciferase was used as a negative control.

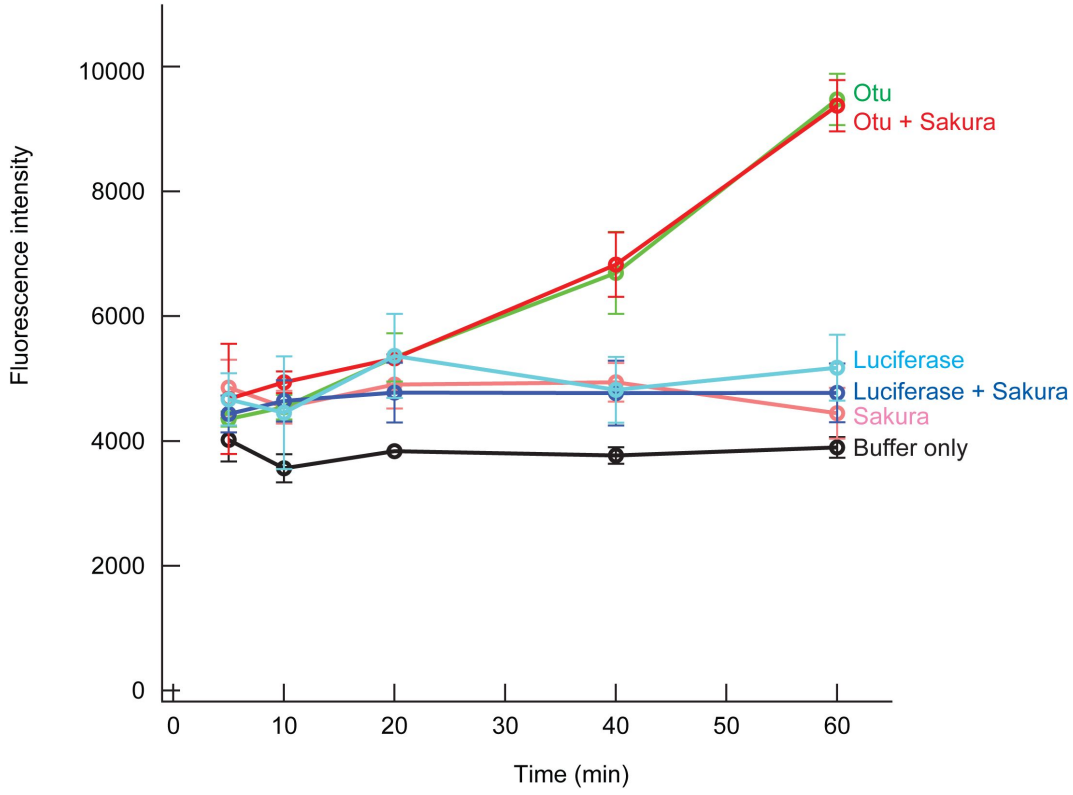

Acknowledgements

We thank Bloomington Drosophila Stock Center, Vienna Drosophila Resource Center, and Kyoto Drosophila Stock Center for fly strain stocks. We thank the Johns Hopkins University School of Medicine Microscope Facility for use of the Zeiss LSM700, supported by NIH grant S10OD016374 awarded to Dr. Scot C. Kuo. We thank Ms. Lauren DeVine and Dr. Bob Cole at the Johns Hopkins University School of Medicine Mass Spectrometry and Proteomics Core Facility for the mass-spec analysis. This work was supported by the grants from the National Institutes of Health [R35GM145352 and R03AI178064] and Johns Hopkins University Catalyst Award to RF.

Additional information

Author Contributions

Methodology and Investigation, A.A., L.Z., and R.F.; Conceptualization and Writing, A.A. and R.F.; Funding Acquisition and Supervision, R.F.

Competing interests

The authors have no conflicts of interest to declare.

Funding

NIGMS (R35GM145352)

NIAID (R03AI178064)

References

Bopp D, Horabin JI, Lersch RA, Cline TW, Schedl P (1993) **Expression of the Sex-lethal gene is controlled at multiple levels during Drosophila oogenesis** *Development* **118**:797–812 Google Scholar

Casanueva MO, Ferguson EL (2004) **Germline stem cell number in the Drosophila ovary is regulated by redundant mechanisms that control Dpp signaling** *Development* **131**:1881–1890 Google Scholar

Chau J, Kulnane LS, Salz HK (2012) **Sex-lethal enables germline stem cell differentiation by down-regulating Nanos protein levels during Drosophila oogenesis** *Proceedings of the National Academy of Sciences of the United States of America* **109**:9465–9470 Google Scholar

Chen D, McKearin D (2003a) **Dpp signaling silences bam transcription directly to establish asymmetric divisions of germline stem cells** *Current biology: CB* **13**:1786–1791 Google Scholar

Chen D, McKearin DM (2003b) **A discrete transcriptional silencer in the bam gene determines asymmetric division of the Drosophila germline stem cell** *Development* **130**:1159–1170 Google Scholar

Chen D, Wang Q, Huang H, Xia L, Jiang X, Kan L, Sun Q, Chen D (2009) **Effete-mediated degradation of Cyclin A is essential for the maintenance of germline stem cells in Drosophila** *Development* **136**:4133–4142 Google Scholar

Chu HP, Liao Y, Novak JS, Hu Z, Merkin JJ, Shymkiv Y, Braeckman BP, Dorovkov MV, Nguyen A, Clifford PM, et al. (2014) **Germline quality control: eEF2K stands guard to eliminate defective oocytes** *Developmental cell* **28**:561–572 Google Scholar

Cox DN, Chao A, Baker J, Chang L, Qiao D, Lin H (1998) **A novel class of evolutionarily conserved genes defined by piwi are essential for stem cell self-renewal** *Genes & development* **12**:3715–3727 Google Scholar

de Cuevas M, Matunis EL (2011) **The stem cell niche: lessons from the Drosophila testis** *Development* **138**:2861–2869 Google Scholar

de Cuevas M, Spradling AC (1998) **Morphogenesis of the Drosophila fusome and its implications for oocyte specification** *Development* **125**:2781–2789 Google Scholar

Donertas D, Sienski G, Brennecke J (2013) **Drosophila Gtsf1 is an essential component of the Piwi-mediated transcriptional silencing complex** *Genes & development* **27**:1693–1705 Google Scholar

Eliazer S, Shalaby NA, Buszczak M (2011) **Loss of lysine-specific demethylase 1 nonautonomously causes stem cell tumors in the Drosophila ovary** *Proceedings of the National Academy of Sciences of the United States of America* **108**:7064–7069 Google Scholar

ElMaghraby MF, Tirian L, Senti KA, Meixner K, Brennecke J (2022) **A genetic toolkit for studying transposon control in the Drosophila melanogaster ovary** *Genetics* **220** Google

Scholar

Fukunaga R, Colpan C, Han BW, Zamore PD (2014) **Inorganic phosphate blocks binding of pre-miRNA to Dicer-2 via its PAZ domain** *The EMBO journal* **33**:371–384 Google Scholar

Fukunaga R, Doudna JA (2009) **dsRNA with 5' overhangs contributes to endogenous and antiviral RNA silencing pathways in plants** *The EMBO journal* **28**:545–555 Google Scholar

Fukunaga R, Han BW, Hung JH, Xu J, Weng Z, Zamore PD (2012) **Dicer partner proteins tune the length of mature miRNAs in flies and mammals** *Cell* **151**:533–546 Google Scholar

Gans M, Audit C, Masson M (1975) **Isolation and Characterization of Sex-Linked Female-Sterile Mutants in Drosophila-Melanogaster** *Genetics* **81**:683–704 Google Scholar

Gateff E, Kurzik-Dumke U, Wismar J, Loffler T, Habtemichael N, Konrad L, Dreschers S, Kaiser S, Protin U (1996) **Drosophila differentiation genes instrumental in tumor suppression** *Int J Dev Biol* **40**:149–156 Google Scholar

Gilboa L, Forbes A, Tazuke SI, Fuller MT, Lehmann R (2003) **Germ line stem cell differentiation in Drosophila requires gap junctions and proceeds via an intermediate state** *Development* **130**:6625–6634 Google Scholar

Glenn LE, Searles LL (2001) **Distinct domains mediate the early and late functions of the Drosophila ovarian tumor proteins** *Mechanisms of development* **102**:181–191 Google Scholar

Gollin SM, King RC (1981) **Studies of Fs(1)1621, a Mutation Producing Ovarian-Tumors in Drosophila-Melanogaster** *Developmental Genetics* **2**:203–218 Google Scholar

Grmai L, Pozmanter C, Van Doren M (2022) **The Regulation of Germline Sex Determination in Drosophila by Sex lethal** *Sex Dev* **16**:323–328 Google Scholar

Handler D, Meixner K, Pizka M, Lauss K, Schmied C, Gruber FS, Brennecke J (2013) **The genetic makeup of the Drosophila piRNA pathway** *Molecular cell* **50**:762–777 Google Scholar

Hayashi Y, Yoshinari Y, Kobayashi S, Niwa R (2020) **The regulation of Drosophila ovarian stem cell niches by signaling crosstalk** *Curr Opin Insect Sci* **37**:23–29 Google Scholar

Hinnant TD, Merkle JA, Ables ET (2020) **Coordinating Proliferation, Polarity, and Cell Fate in the Drosophila Female Germline** *Front Cell Dev Biol* **8**:19 Google Scholar

Huang X, Fejes Toth K, Aravin AA (2017) **piRNA Biogenesis in Drosophila melanogaster** *Trends Genet* **33**:882–894 Google Scholar

Ji S, Li C, Hu L, Liu K, Mei J, Luo Y, Tao Y, Xia Z, Sun Q, Chen D (2017) **Bam-dependent deubiquitinase complex can disrupt germ-line stem cell maintenance by targeting cyclin A** *Proceedings of the National Academy of Sciences of the United States of America* **114**:6316–6321 Google Scholar

Ji S, Luo Y, Cai Q, Cao Z, Zhao Y, Mei J, Li C, Xia P, Xie Z, Xia Z, et al. (2019) **LC Domain-Mediated Coalescence Is Essential for Otu Enzymatic Activity to Extend Drosophila Lifespan** *Molecular cell* **74**:363–377 Google Scholar

Jin Z, Flynt AS, Lai EC (2013) **Drosophila piwi mutants exhibit germline stem cell tumors that are sustained by elevated Dpp signaling** *Current biology: CB* **23**:1442–1448 Google

Scholar

Jumper J, Evans R, Pritzel A, Green T, Figurnov M, Ronneberger O, Tunyasuvunakool K, Bates R, Zidek A, Potapenko A, et al. (2021) **Highly accurate protein structure prediction with AlphaFold** *Nature* **596**:583–589 Google Scholar

Kahney EW, Snedeker JC, Chen X (2019) **Regulation of Drosophila germline stem cells** *Current opinion in cell biology* **60**:27–35 Google Scholar

Kai T, Spradling A (2003) **An empty Drosophila stem cell niche reactivates the proliferation of ectopic cells** *Proceedings of the National Academy of Sciences of the United States of America* **100**:4633–4638 Google Scholar

Kandasamy SK, Fukunaga R (2016) **Phosphate-binding pocket in Dicer-2 PAZ domain for high-fidelity siRNA production** *Proceedings of the National Academy of Sciences of the United States of America* **113**:14031–14036 Google Scholar

Kandasamy SK, Zhu L, Fukunaga R (2017) **The C-terminal dsRNA-binding domain of Drosophila Dicer-2 is crucial for efficient and high-fidelity production of siRNA and loading of siRNA to Argonaute2** *Rna* **23**:1139–1153 Google Scholar

Kang I, Choi Y, Jung S, Lim JY, Lee D, Gupta S, Moon W, Shin C (2018) **Identification of target genes regulated by the Drosophila histone methyltransferase Eggless reveals a role of Decapentaplegic in apoptotic signaling** *Scientific reports* **8**:7123 Google Scholar

King RC, Mohler D, Riley SF, Storto PD, Nicolazzo PS (1986) **Complementation between alleles at the ovarian tumor locus of Drosophila melanogaster** *Dev Genet* **7**:1–20 Google Scholar

King RC, Riley SF (1982) **Ovarian Pathologies Generated by Various Alleles of the Otu Locus in Drosophila-Melanogaster** *Developmental Genetics* **3**:69–89 Google Scholar

Kirilly D, Xie T (2007) **The Drosophila ovary: an active stem cell community** *Cell research* **17**:15–25 Google Scholar

Levin HL, Moran JV (2011) **Dynamic interactions between transposable elements and their hosts** *Nature Reviews Genetics* **12**:615–627 Google Scholar

Li Y, Minor NT, Park JK, McKearin DM, Maines JZ (2009) **Bam and Bgcn antagonize Nanos-dependent germ-line stem cell maintenance** *Proceedings of the National Academy of Sciences of the United States of America* **106**:9304–9309 Google Scholar

Li Y, Zhang Q, Carreira-Rosario A, Maines JZ, McKearin DM, Buszczak M (2013) **Mei-p26 cooperates with Bam, Bgcn and Sxl to promote early germline development in the Drosophila ovary** *PloS one* **8**:e58301 Google Scholar

Liao SE, Ai Y, Fukunaga R (2018) **An RNA-binding protein Blanks plays important roles in defining small RNA and mRNA profiles in Drosophila testes** *Heliyon* **4**:e00706 Google Scholar

Liao SE, Kandasamy SK, Zhu L, Fukunaga R (2019) **DEAD-box RNA helicase Belle post-transcriptionally promotes gene expression in an ATPase activity-dependent manner** *Rna* Google Scholar

Lin H (1997) **The tao of stem cells in the germline** *Annu Rev Genet* **31**:455–491 Google Scholar

Lin H, Spradling AC (1993) **Germline stem cell division and egg chamber development in transplanted Drosophila germaria** *Developmental biology* **159**:140–152 Google Scholar

Losick VP, Morris LX, Fox DT, Spradling A (2011) **Drosophila stem cell niches: a decade of discovery suggests a unified view of stem cell regulation** *Developmental cell* **21**:159–171 Google Scholar

McKearin D, Ohlstein B (1995) **A role for the Drosophila bag-of-marbles protein in the differentiation of cystoblasts from germline stem cells** *Development* **121**:2937–2947 Google Scholar

McKearin DM, Spradling AC (1990) **. bag-of-marbles: a Drosophila gene required to initiate both male and female gametogenesis** *Genes & development* **4**:2242–2251 Google Scholar

Moon S, Cassani M, Lin YA, Wang L, Dou K, Zhang ZZ (2018) **A Robust Transposon-Endogenizing Response from Germline Stem Cells** *Developmental cell* **47**:660–671 Google Scholar

Ohlstein B, Lavoie CA, Vef O, Gateff E, McKearin DM (2000) **The Drosophila cystoblast differentiation factor, benign gonial cell neoplasm, is related to DExH-box proteins and interacts genetically with bag-of-marbles** *Genetics* **155**:1809–1819 Google Scholar

Ohlstein B, McKearin D (1997) **Ectopic expression of the Drosophila Bam protein eliminates oogenic germline stem cells** *Development* **124**:3651–3662 Google Scholar

Ohtani H, Iwasaki YW, Shibuya A, Siomi H, Siomi MC, Saito K (2013) **DmGTSF1 is necessary for Piwi-piRISC-mediated transcriptional transposon silencing in the Drosophila ovary** *Genes & development* **27**:1656–1661 Google Scholar

Ota R, Kobayashi S (2020) **Myc plays an important role in Drosophila P-M hybrid dysgenesis to eliminate germline cells with genetic damage** *Commun Biol* **3**:185 Google Scholar

Pauli D, Oliver B, Mahowald AP (1993) **The role of the ovarian tumor locus in Drosophila melanogaster germ line sex determination** *Development* **119**:123–134 Google Scholar

Pek JW, Lim AK, Kai T (2009) **Drosophila maelstrom ensures proper germline stem cell lineage differentiation by repressing microRNA-7** *Developmental cell* **17**:417–424 Google Scholar

Penalva LO, Sanchez L (2003) **RNA binding protein sex-lethal (Sxl) and control of Drosophila sex determination and dosage compensation** *Microbiology and molecular biology reviews: MMBR* **67**:343–359 Google Scholar

Rodesch C, Pettus J, Nagoshi RN (1997) **The Drosophila ovarian tumor gene is required for the organization of actin filaments during multiple stages in oogenesis** *Developmental biology* **190**:153–164 Google Scholar

Rubin T, Huynh JR (2015) **Mosaic Analysis in the Drosophila melanogaster Ovary** *Methods in molecular biology* **1328**:29–55 Google Scholar

Salz HK, Erickson JW (2010) **Sex determination in Drosophila: The view from the top** *Fly* **4**:60–70 Google Scholar

Sass GL, Comer AR, Searles LL (1995) **The ovarian tumor protein isoforms of Drosophila melanogaster exhibit differences in function, expression, and localization** *Developmental biology* **167**:201–212 Google Scholar

Siomi MC, Sato K, Pezic D, Aravin AA (2011) **PIWI-interacting small RNAs: the vanguard of genome defence** *Nature reviews Molecular cell biology* **12**:246–258 Google Scholar

Smith PA, King RC (1966) **Studies on Fused a Mutant Gene Producing Ovarian Tumors in Drosophila Melanogaster** *Genetics* **54**:363 Google Scholar

Song X, Wong MD, Kawase E, Xi R, Ding BC, McCarthy JJ, Xie T (2004) **Bmp signals from niche cells directly repress transcription of a differentiation-promoting gene, bag of marbles, in germline stem cells in the Drosophila ovary** *Development* **131**:1353–1364 Google Scholar

Song X, Zhu CH, Doan C, Xie T (2002) **Germline stem cells anchored by adherens junctions in the Drosophila ovary niches** *Science* **296**:1855–1857 Google Scholar

Steinhauer WR, Kalfayan LJ (1992a) **A specific ovarian tumor protein isoform is required for efficient differentiation of germ cells in Drosophila oogenesis** *Genes & development* **6**:233–243 Google Scholar

Steinhauer WR, Kalfayan LJ (1992b) **A Specific Ovarian Tumor Protein Isoform Is Required for Efficient Differentiation of Germ-Cells in Drosophila Oogenesis** *Genes & development* **6**:233–243 Google Scholar

Storto PD, King RC (1987) **Fertile heteroallelic combinations of mutant alleles of the otu locus of Drosophila melanogaster** *Rouxs Arch Dev Biol* **196**:210–221 Google Scholar

Storto PD, King RC (1988) **Multiplicity of functions for the otu gene products during Drosophila oogenesis** *Dev Genet* **9**:91–120 Google Scholar

Van Buskirk C, Schupbach T (2002) **Half pint regulates alternative splice site selection in Drosophila** *Developmental cell* **2**:343–353 Google Scholar

Wang Z, Lin H (2004) **Nanos maintains germline stem cell self-renewal by preventing differentiation** *Science* **303**:2016–2019 Google Scholar

Xia L, Jia S, Huang S, Wang H, Zhu Y, Mu Y, Kan L, Zheng W, Wu D, Li X, et al. (2010) **The Fused/Smurf complex controls the fate of Drosophila germline stem cells by generating a gradient BMP response** *Cell* **143**:978–990 Google Scholar

Xie T, Spradling AC (1998) **. decapentaplegic is essential for the maintenance and division of germline stem cells in the Drosophila ovary** *Cell* **94**:251–260 Google Scholar

Xu T, Rubin GM (1993) **Analysis of genetic mosaics in developing and adult Drosophila tissues** *Development* **117**:1223–1237 Google Scholar

Yamashiro H, Siomi MC (2018) **PIWI-Interacting RNA in Drosophila: Biogenesis, Transposon Regulation, and Beyond** *Chem Rev* **118**:4404–4421 Google Scholar

Yang F, Quan Z, Huang H, He M, Liu X, Cai T, Xi R (2019) **Ovaries absent links dLsd1 to HP1a for local H3K4 demethylation required for heterochromatic gene silencing** *eLife* **8** Google Scholar

Yang L, Chen D, Duan R, Xia L, Wang J, Qurashi A, Jin P, Chen D (2007) **Argonaute 1 regulates the fate of germline stem cells in Drosophila** *Development* **134**:4265–4272 Google Scholar

Yang Z, Zeng X, Zhao Y, Chen R (2023) **AlphaFold2 and its applications in the fields of biology and medicine** *Signal Transduct Target Ther* **8**:115 Google Scholar

Zhu L, Fukunaga R (2021) **RNA-binding protein Maca is crucial for gigantic male fertility factor gene expression, spermatogenesis, and male fertility, in Drosophila** *PLoS genetics* **17**:e1009655 Google Scholar

Zhu L, Kandasamy SK, Fukunaga R (2018a) **Dicer partner protein tunes the length of miRNAs using base-mismatch in the pre-miRNA stem** *Nucleic acids research* Google Scholar

Zhu L, Kandasamy SK, Liao SE, Fukunaga R (2018b) **LOTUS domain protein MARF1 binds CCR4-NOT deadenylase complex to post-transcriptionally regulate gene expression in oocytes** *Nature communications* **9**:4031 Google Scholar

Zhu L, Liao SE, Ai Y, Fukunaga R (2019a) **RNA methyltransferase BCDIN3D is crucial for female fertility and miRNA and mRNA profiles in Drosophila ovaries** *PloS one* **14**:e0217603 Google Scholar

Zhu L, Liao SE, Fukunaga R (2019b) **Drosophila Regnase-1 RNase is required for mRNA and miRNA profile remodelling during larva-to-adult metamorphosis** *RNA biology* **16**:1386–1400 Google Scholar

Author information

Azali Azlan
Department of Biological Chemistry, Johns Hopkins School of Medicine, Baltimore, United States

Li Zhu
Department of Biological Chemistry, Johns Hopkins School of Medicine, Baltimore, United States

Ryuya Fukunaga
Department of Biological Chemistry, Johns Hopkins School of Medicine, Baltimore, United States
ORCID iD: 0000-0002-5814-8206

For correspondence: fukunaga@jhmi.edu

Editors

Reviewing Editor
Olivia Rissland
University of Colorado School of Medicine, Aurora, United States of America

Senior Editor
Sofia Araújo
University of Barcelona, Barcelona, Spain

Reviewer #1 (Public review):

In this manuscript, Azlan et al. identified a novel maternal factor called Sakura that is required for proper oogenesis in Drosophila. They showed that Sakura is specifically expressed in the female germline cells. Consistent with its expression pattern, Sakura functioned autonomously in germline cells to ensure proper oogenesis. In sakura KO flies, germline cells were lost during early oogenesis and often became tumorous before degenerating by apoptosis. In these tumorous germ cells, piRNA production was defective and many transposons were derepressed. Interestingly, Smad signaling, a critical signaling pathway for the GSC maintenance, was abolished in sakura KO germline stem cells, resulting in ectopic expression of Bam in whole germline cells in the tumorous germline. A recent study reported that Bam acts together with the deubiquitinase Otu to stabilize Cyc A. In the absence of sakura, Cyc A was upregulated in tumorous germline cells in the germarium. Furthermore, the authors showed that Sakura co-immunoprecipitated Otu in ovarian extracts. A series of in vitro assays suggested that the Otu (1-339 aa) and Sakura (1-49 aa) are sufficient for their direct interaction. Finally, the authors demonstrated that the loss of otu phenocopies the loss of sakura, supporting their idea that Sakura plays a role in germ cell maintenance and differentiation through interaction with Otu during oogenesis.

Latest comments:

The reviewer acknowledges the importance of sharing the observed defects in Sakura mutant ovaries and the possible physiological significance of the Sakura-Out interaction with the research community, as this information could lay the groundwork for future functional analysis research.

https://doi.org/10.7554/eLife.103828.3.sa3

Reviewer #2 (Public review):

In this study, the authors identified CG14545 (named it sakura), as a key gene essential for Drosophila oogenesis. Genetic analyses revealed that Sakura is vital for both oogenesis progression and ultimate female fertility, playing a central role in the renewal and differentiation of germ stem cells (GSC).

The absence of Sakura disrupts the Dpp/BMP signaling pathway, resulting in abnormal bam gene expression, which impairs GSC differentiation and leads to GSC loss. Additionally, Sakura is critical for maintaining normal levels of piRNAs. Also, the authors convincingly demonstrate that Sakura physically interacts with Otu, identifying the specific domains necessary for this interaction, suggesting a cooperative role in germline regulation. Importantly, the loss of otu produces similar defects to those observed in sakura mutants, highlighting their functional collaboration.

The authors provide compelling evidence that Sakura is a critical regulator of germ cell fate, maintenance, and differentiation in Drosophila. This regulatory role is mediated through modulation of pMad and Bam expression. However, the phenotypes observed in the germarium appear to stem from reduced pMad levels, which subsequently trigger premature and ectopic expression of Bam. This aberrant Bam expression could lead to increased CycA levels and altered transcriptional regulation, impacting piRNA expression. In this revised manuscript, the authors further investigated whether Sakura affects the function of Orb, a binding partner they identified, in deubiquitinase activity when Orb interacts with Bam.

This elaborate study will be embraced by both germline-focused scientists and the developmental biology community.

Latest comments:

The authors answered all my persistent concerns and made changes according to the recommendations I incorporated for the revised version of the manuscript.

https://doi.org/10.7554/eLife.103828.3.sa2

Reviewer #3 (Public review):

In this very thorough study, the authors characterize the function of a novel Drosophila gene, which they name Sakura. They start with the observation that sakura expression is predicted to be highly enriched in the ovary and they generate an anti-sakura antibody, a line with a GFP-tagged sakura transgene, and a sakura null allele to investigate sakura localization and function directly. They confirm the prediction that it is primarily expressed in the ovary and, specifically, that it is expressed in germ cells, and find that about 2/3 of the mutants lack germ cells completely and the remaining have tumorous ovaries. Further investigation reveals that Sakura is required for piRNA-mediated repression of transposons in germ cells. They also find evidence that sakura is important for germ cell specification during development and germline stem cell maintenance during adulthood. However, despite the role of sakura in maintaining germline stem cells, they find that sakura mutant germ cells also fail to differentiate properly such that mutant germline stem cell clones have an increased number of "GSC-like" cells. They attribute this phenotype to a failure in the repression of Bam by dpp signaling. Lastly, they demonstrate that sakura physically interacts with otu and that sakura and otu mutants have similar germ cell phenotypes. Overall, this study helps to advance the field by providing a characterization of a novel gene that is required for oogenesis. The data are generally high-quality and the new lines and reagents they generated will be useful for the field.

Latest comments:

As with my previous assessment, I remain supportive of publication of this manuscript. Though I agree with the other reviewers that additional experimentation would increase the value of this study even further, I feel it will also be a useful contribution to the field as is.

https://doi.org/10.7554/eLife.103828.3.sa1

Author response:

The following is the authors' response to the previous reviews

Public Reviews:

Reviewer #1 (Public review):

Summary:

In this manuscript, Azlan et al. identified a novel maternal factor called Sakura that is required for proper oogenesis in Drosophila. They showed that Sakura is specifically expressed in the female germline cells. Consistent with its expression pattern, Sakura functioned autonomously in germline cells to ensure proper oogenesis. In sakura KO flies, germline cells were lost during early oogenesis and often became tumorous before degenerating by apoptosis. In these tumorous germ cells, piRNA production was defective and many transposons were derepressed. Interestingly, Smad signaling, a critical signaling pathway for the GSC maintenance, was abolished in sakura KO germline stem cells, resulting in ectopic expression of Bam in whole germline cells in the tumorous germline. A recent study reported that Bam acts together with the deubiquitinase Otu to stabilize Cyc A. In the absence of sakura, Cyc A was upregulated in tumorous germline cells in the germarium. Furthermore, the authors showed that Sakura co-immunoprecipitated Otu in ovarian extracts. A series of in vitro assays suggested that the Otu (1-339 aa) and Sakura (1-49 aa) are sufficient for their direct interaction. Finally, the authors demonstrated that the loss of otu phenocopies the loss of sakura, supporting their idea that Sakura plays a role in germ cell maintenance and differentiation through interaction with Otu during oogenesis.

Strengths:

To my knowledge, this is the first characterization of the role of CG14545 genes. Each experiment seems to be well-designed and adequately controlled

Weaknesses:

However, the conclusions from each experiment are somewhat separate, and the functional relationships between Sakura's functions are not well established. In other words, although the loss of Sakura in the germline causes pleiotropic effects, the cause-and-effect relationships between the individual defects remain unclear.

Comments on latest version:

The authors have attempted to address my initial concerns with additional experiments and refutations. Unfortunately, my concerns, especially my specific comments 1-3, remain unaddressed. The present manuscript is descriptive and fails to describe the molecular mechanism by which Sakura exerts its function in the germline. Nevertheless, this reviewer acknowledges that the observed defects in sakura mutant ovaries and the possible physiological significance of the Sakura-Out interaction are worth sharing with the research community, as they may lay the groundwork for future research in functional analysis.

We thank the reviewer for valuable comments. We would like to investigate the molecular mechanism by which Sakura exerts its function in the germline in near future studies.

Reviewer #2 (Public review):

In this study, the authors identified CG14545 (named it sakura), as a key gene essential for Drosophila oogenesis. Genetic analyses revealed that Sakura is vital for both oogenesis progression and ultimate female fertility, playing a central role in the renewal and differentiation of germ stem cells (GSC).

> *The absence of Sakura disrupts the Dpp/BMP signaling pathway, resulting in abnormal bam gene expression, which impairs GSC differentiation and leads to GSC loss. Additionally, Sakura is critical for maintaining normal levels of piRNAs. Also, the authors convincingly demonstrate that Sakura physically interacts with Otu, identifying the specific domains necessary for this interaction, suggesting a cooperative role in germline regulation. Importantly, the loss of otu produces similar defects to those observed in sakura mutants, highlighting their functional collaboration.*
>
> *The authors provide compelling evidence that Sakura is a critical regulator of germ cell fate, maintenance, and differentiation in Drosophila. This regulatory role is mediated through modulation of pMad and Bam expression. However, the phenotypes observed in the germarium appear to stem from reduced pMad levels, which subsequently trigger premature and ectopic expression of Bam. This aberrant Bam expression could lead to increased CycA levels and altered transcriptional regulation, impacting piRNA expression. In this revised manuscript, the authors further investigated whether Sakura affects the function of Orb, a binding partner they identified, in deubiquitinase activity when Orb interacts with Bam.*
>
> *We appreciate the authors' efforts to address all our comments. While these revisions have greatly improved the clarity of certain sections, some of the concerns remain unclear, while details mentioned in the responses about these studies should be incorporated in the manuscript. Specifically, the manuscript still lacks the demonstration that Sakura co-localizes with Orb/Bam despite having the means for staining and visualization. This would bring insight into the selective binding of Orb with Bam vs. Sakura perhaps at different stages of oogenesis. Such analyses would allow for more specific conclusions, further alluding to the underlying mechanism, rather than the general observations currently presented.*
>
> *This elaborate study will be embraced by both germline-focused scientists and the developmental biology community.*

We thank the reviewer for valuable comments. We believe that the author meant Otu, not Orb, for the binding partner of Sakura that we identified. We would like to investigate the colocalization of Sakura with other proteins including Otu and the molecular mechanism by which Sakura exerts its function in the germline in near future studies.

> ***Reviewer #3 (Public review):***
>
> *In this very thorough study, the authors characterize the function of a novel Drosophila gene, which they name Sakura. They start with the observation that sakura expression is predicted to be highly enriched in the ovary and they generate an anti-sakura antibody, a line with a GFP-tagged sakura transgene, and a sakura null allele to investigate sakura localization and function directly. They confirm the prediction that it is primarily expressed in the ovary and, specifically, that it is expressed in germ cells, and find that about 2/3 of the mutants lack germ cells completely and the remaining have tumorous ovaries. Further investigation reveals that Sakura is required for piRNA-mediated repression of transposons in germ cells. They also find evidence that sakura is important for germ cell specification during development and germline stem cell maintenance during adulthood. However, despite the role of sakura in maintaining germline stem cells, they find that sakura mutant germ cells also fail to differentiate properly such that mutant germline stem cell clones have an increased number of "GSC-like" cells. They attribute this phenotype to a failure in the repression of Bam by dpp signaling. Lastly, they demonstrate that sakura physically interacts with otu and that sakura and otu mutants have similar germ cell phenotypes. Overall, this study helps to advance the field by providing a characterization of a novel gene that is required for oogenesis. The data*

> *are generally high-quality and the new lines and reagents they generated will be useful for the field.*
>
> *Comments on latest version:*
>
> *With these revisions, the authors have addressed my main concerns.*

We thank the reviewer for valuable comments.

> ***Recommendations for the authors:***
>
> ***Reviewer #2 (Recommendations for the authors):***
>
> *The manuscript is much improved based on the changes made upon recommendations from the reviewers.*
>
> *Though most of our comments have been addressed, we have a few more we wish to recommend. For previous points we made, we replied with further clarification for the authors.*
>
> *Figure 1*
>
> *(1) B should be the supplemental figure.*
>
> *We moved the former Fig 1B to Supplemental Figure 1.*
>
> *• Previous Fig1B (sakura mRNA expression level) is now Fig S2, not S1. Please make this data as Fig S1.*

We moved Fig S1 to main Fig7A and renumbered Fig S2-S16 to Fig S1-S15.

> *(2) C - How were the different egg chamber stages selected in the WB? Naming them 'oocytes' is deceiving. Recommend labeling them as 'egg chambers', since an oocyte is claimed to be just the one-cell of that cyst.*
>
> *We changed the labeling to egg chambers.*
>
> *• The labels on lanes for Stages 12-13 and Stage 14, still only say "chambers", not "egg chambers". Also there is no Stage 1-3 egg chamber. More accurately, the label should be "Germarium - Stage 11 egg chambers".*

We updated the lables on lanes as suggested by the reviewer.

> *(3) Is the antibody not detecting Sakura in IF? There is no mention of this anywhere in the manuscript.*
>
> *While our Sakura antibody detects Sakura in IF, it seems to detect some other proteins as well. Since we have Sakura-EGFP fly strain (which fully rescues sakuranull phenotypes) to examine Sakura expression and localization without such non-specific signal issues, we relied on Sakura-EGFP rather than anti-Sakura antibodies for IF.*
>
> *• Please put this info into the Methods section.*

We added this info into the Methods section.

> *(4) Expand on the reliance of the sakura-EGFP fly line. Does this overexpression cause any phenotypes?*

> *sakura-EGFP does not cause any phenotypes in the background of sakura[+/+] and sakura[+/-].*
>
> *• Please add this detail into the manuscript.*

We added this info into the Methods section.

> *Figure 5*
>
> *(1) D - It might make more sense if this graph showed % instead of the numbers.*
>
> *We did not understand the reviewer's point. We think using numbers, not %, makes more sense.*
>
> *• Having a different 'n' number for each experiment does not allow one to compare anything except numbers of the egg chambers. This must be normalized.*

We still don't agree with the reviewer. In Fig 5D, we are showing the numbers of stage 14 oocytes per fly (= per a pair of ovaries). 'n' is the number of flies (= number of a pair of ovaries) examined. We now clarified this in the figure legend. Different 'n' number does not prevent us from comparing the numbers of stage 14 oocytes per fly. Therefore, we would like to show as it is now.

> *(2) Line 213 - explain why RNAi 2 was chosen when RNAi 1 looks stronger.*
>
> *Fly stock of RNAi line 2 is much healthier than RNAi line 1 (without being driven Gal4) for some reasons. We had a concern that the RNAi line 1 might contain an unwanted genetic background. We chose to use the RNAi 2 line to avoid such an issue.*
>
> *• Please add this information to the manuscript.*

We added this info into the Methods section.

> *Figure 7/8 - can go to Supplemental.*
>
> *We moved Fig 8 to supplemental. However, we think Fig 7 data is important and therefore we would like to present them as a main figure.*
>
> *• Current Fig S1 should go to Fig 7, to better understand the relationship between pMad and Bam expression.*

We moved Fig S1 to main Fig7A and renumbered Fig S2-S16 to Fig S1-S15.

> *Figure 9C - Why the switch to S2 cells? Not able to use the Otu antibody in the IP of ovaries?*
>
> *We can use the Otu antibody in the IP of ovaries. However, in anti-Sakura Western after anti Otu IP, antibody light chain bands of the Otu antibodies overlap with the Sakura band. Therefore, we switched to S2 cells to avoid this issue by using an epitope tag.*
>
> *• Please add this info to the Methods section.*

We added this info into the Methods section.

> *Figure 10- Some images would be nice here to show that the truncations no longer colocalize.*

> *We did not understand the reviewer's points. In our study, even for the full-length proteins. We have not shown any colocalization of Sakura and Otu in S2 cells or in ovaries, except that they both are enriched in developing oocytes in egg chambers.*
>
> *• Based on your binding studies, we would expect them to colocalize in the egg chamber, and since there are antibodies and a GFP-line available, it would be important to demonstrate that via visualization.*

As we wrote in the response and now in the manuscript, our antibodies are not best for immunostaining. We will try to optimize the experimental conditions in the future studies.

https://doi.org/10.7554/eLife.103828.3.sa0